Am J Cancer Res 2021;11(2):416-440
www.ajcr.us /ISSN:2156-6976/ajcr0116634

Original Article

YEATS4 is associated with poor prognosis and promotes epithelial-to-mesenchymal transition and metastasis by regulating ZEB1 expression in breast cancer

Yang Li, Lei Li, Junyi Wu, Jun Qin, Xueming Dai, Tao Jin, Junming Xu

Department of General Surgery, Shanghai General Hospital, Shanghai Jiao Tong University School of Medicine, Shanghai 200080, China

Received June 19, 2020; Accepted December 4, 2020; Epub February 1, 2021; Published February 15, 2021

Abstract: YEATS domain-containing protein 4 (YEATS4) is implicated in several oncogenic signaling pathways, and its expression is involved in various types of cancer; regardless, the pathophysiologic effects of YEATS4 on breast cancer remain unclear. This study finds that YEATS4 is increasingly expressed with breast cancer progression, and its expression is related to poor outcome and distant metastasis. YEATS4 overexpression in breast cancer cells strengthens their malignant characteristics *in vitro* and *in vivo*, particularly inducing epithelial-to-mesenchymal transition (EMT) and consequently, metastatic capability in breast cancer cells. By contrast, deleting YEATS4 in breast cancer cells with high-grade malignancy reduced these characteristics. With regard to the molecular mechanism, YEATS4 mediates histone H3K27ac at specific sites of the ZEB1 promoter to regulate its expression at the transcription level. Depleting ZEB1 blocks YEATS4-induced EMT, migration, invasion, and metastasis. YEATS4 expression is also positively correlated with ZEB1 expression in patients with breast cancer. Co-expression of YEATS4 and ZEB1 correlates with the shortest distant metastasis-free period. Taken together, our data reveal the critical role of YEATS4 in the progression and metastasis of breast cancer, as well as support YEATS4 as a potential therapeutic target and prognostic biomarker for breast cancer.

Keywords: YEATS4, ZEB1, breast cancer, EMT, metastasis

Introduction

Breast cancer is one of the most common malignancies with a rising incidence rate and the highest cancer mortality rate in females worldwide. An estimated 2.1 million new cases and 626,679 deaths were reported in 2018 [1, 2]. Despite various methods for early diagnosis and multidisciplinary treatment to lower mortality rates [3], 25%-50% of breast cancer patients were predicted to ultimately develop distant metastases and then succumbed after decades of diagnosis and primary tumor resection [4, 5].

Treatment modalities for breast cancer metastasis have thus far remained ineffective. Considerable efforts have been directed toward exploring the mechanisms of metastasis to identify a more effective treatment for breast cancer distant metastasis. The mechanism by which, metastasis occurs has yet to be determined. Accumulating evidence indicates that epithelial-to-mesenchymal transition (EMT), marked by loss of epithelial properties and acquisition of mesenchymal phenotypes, endows cancer cells with more aggressive behavior [6-8]. Thus, potential molecules in the adjustment of EMT need to be confirmed to identify new therapeutic targets for breast cancer progression and metastasis.

YEATS domain-containing protein 4 (YEATS4) located in the chromosomal region 12q13-15 has been initially identified in the nucleoli of glioma cells [9]. As a member of the protein family with a characteristic YEATS domain at the N-terminal [10], YEATS4 participates in chromatin modification and transcription regulation by involving the assembly of multisubunit complexes, particularly TIP60/TRRAP and SRCAP complexes [11, 12], mediating histone

proteins to participate in nucleosome remodeling, changing chromatin composition, and affecting gene transcription [13]. In multiple types of cancer, YEATS4 has been implicated in the progression of several types of cancer, including pancreatic cancer, gastric cancer, colorectal cancer, hepatocellular carcinoma, and non-small cell lung cancer [14-19]. Kim et al. also reported that YEATS4 is one of the key transcription factors inducing chemoresistance via intrinsic apoptosis-related pathways in ovarian cancer [20]. However, the pathophysiologic effects of YEATS4 on breast cancer remain unclear. Moreover, most of these studies have focused on the promoting effect of YEATS4 on cell proliferation. Whether and how YEATS4 contributes to cancer invasion and metastasis remains undetermined.

In the current study, we reveal that YEATS4 overexpression promotes proliferation and EMT in breast cancer cells, leading to aggressive phenotypes *in vitro* and *in vivo*. YEATS4 deletion restrains cell growth, results in mesenchymal-to-epithelial transition (MET), and inhibits metastases to distant sites. These effects on biological behavior are achieved by regulating ZEB1 transcription via H3K27 acetylation (H3K27ac). These results show the innovative role of YEATS4 in breast cancer progression and metastasis and provide a rational interpretation of the association of positive YEATS4 expression with progression and poor outcome. Thus, YEATS4 can be used as a potential therapeutic target for breast cancer.

Material and methods

Ethics statement

This experimental research relating to human beings and animals was authorized by the Ethical Review Committee of Shanghai General Hospital, Shanghai Jiao Tong University School of Medicine. Written consent was obtained from each participant before the experiments.

Antibodies and reagents

Antibodies against histone H3, H3K4ac, H3K9ac, H3K14ac, H3K18ac, and H3K27ac were purchased from Abcam. E-cadherin, ZO-1, vimentin, N-cadherin, ZEB1, and GPADH were supplied by Cell Signaling Technology. YEATS4 were provided by Sigma-Aldrich. TRizol LS Reagent was purchased from Invitrogen. X-tremeGENE™ HP DNA Transfection Reagent was supplied by Roche.

Patients and specimens

The retrospective cohort consisted of 481 patients with stages I-III breast cancer who were diagnosed and enrolled in our research from 2005 to 2009 at the Shanghai General Hospital, Shanghai Jiao Tong University School of Medicine, Shanghai, China. The total number included 42 cases of ductal carcinoma *in situ* (DCIS) and 439 cases of invasive carcinoma (IC), as well as 139 paired adjacent normal tissues (ANTs). Notably, 197 patients had lymph node metastasis in this retrospective cohort.

Overall survival (OS) is defined as the number of days after surgery to death from any cause. Distant metastasis-free survival (DMFS) is defined as the period after surgery to the date of diagnosis of distant metastasis derived from breast cancer. The follow-up deadline is the date of death, date of emigration, or September 30, 2019.

The following were the inclusion criteria: (1) Patients were diagnosed with unilateral breast cancer, which was pathologically confirmed. ANTs were pathologically sampled more than 5 cm from the margin of the tumor. (2) Complete clinicopathologic and follow-up data were available. The following were the exclusion criteria: (1) Patients with preoperative anticancer treatment such as radiotherapy, chemotherapy, and hormonal therapy were excluded. (2) Patients with severe complicating diseases such as heart and cerebral vascular diseases or other primary or familial malignancies were ruled out.

Immunohistochemistry

Sections of whole-tissue blocks from 481 breast cancer tissues and 139 ANTs were sliced into 4 μm sections and baked in a heat chamber for 1 h at 60°C. Deparaffination and antigen retrieval were conducted using the PT Link system (Agilent/Dako A/S). Slides were then immunoreacted for 1 h with the anti-YEATS4 primary antibody (diluted at 1:100; Sigma-Aldrich) or the anti-ZEB1 primary antibody (diluted at 1:100; Cell Signaling Technology) and then with a secondary antibody for 30 min. The OptiView DAB IHC Detection Kit

(Ventana Medical Systems) was used for chromogen detection. Hematoxylin was used for counterstaining. The staining intensities and percentages of the positive cells were evaluated by 2 senior pathologists blinded to patient medical information. The staining intensity was graded as 0 (no stain), 1 (weak), 2 (moderate), or 3 (strong). The percentage of positive cancer cells was graded as 0 (< 5%), 1 (5%-25%), 2 (26%-50%), 3 (51%-75%), or 4 (> 75%). YEATS4 or ZEB1 expression was determined based on the semiquantitative immunoreactive score (IRS) [21], which was determined by multiplying the staining intensity with the percentage of positive cells. Slices with scores ranging from 0 to 5 were classified as negative for YEATS4 and ZEB1 expression, whereas those with scores from 6 to 12 were regarded as positive for YEATS4 and ZEB1 expression.

Cell lines and culture conditions

Human breast cancer cell lines MDA-MB-231, BT-474, MCF-7, ZR-75-1, T-47D, SK-BR-3, and MDA-MB-436 and human embryonic kidney cells 293T were obtained from the National Infrastructure of Cell Line Resource (Shanghai, China). The aforementioned cell lines were detected to ensure the absence of mycoplasma contamination. MDA-MB-231 and MDA-MB-436 cells were grown in Leibovitz's L-15 Medium (ATCC), BT-474, ZR-75-1, T-47D, and SK-BR-3 cells in RPMI 1640 (Gibco), MCF-7 cells in Eagle's Minimum Essential Medium (ATCC), and 293T cells in DMEM (Gibco). A base culture medium was added with fetal bovine serum (final concentration: 10%; Gibco), 1% penicillin-streptomycin, and 2 mM L-glutamine. All cell lines were cultured at 37°C in a humidified atmosphere with 5% CO_2.

Lentiviral construction and cell infection

Lentiviral construction and cell infection assays are described in detail in Supplementary materials and methods. The shRNA sequences are listed in Table S1.

RNA isolation and real-time quantitative polymerase chain reaction

Total RNA was extracted using TRIzol™ Reagent (Invitrogen) in accordance with the protocol. Real-time quantitative polymerase chain reaction (RT-qPCR) was conducted using SYBR™ Green PCR Master Mix (Applied Biosystem™), following the instructions provided by the manufacturer. The primer sequences for RT-qPCR are listed in Table S1.

Cell proliferation assays

Cell proliferation assays were conducted as elaborately described in Supplementary materials and methods.

Colony formation and soft agar colony formation assays

Colony formation and soft agar colony formation assays are described in Supplementary materials and methods.

Wound healing assays

Wound healing assays are described in Supplementary materials and methods.

Transwell assays

Transwell-24 well plates (Corning) with a chamber pore size measuring 8 μm were used to perform cell migration and invasion assays. Procedures are elaborately described in Supplementary materials and methods.

Western blot analysis

Western blot analysis was conducted as described in Supplementary materials and methods.

Immunofluorescence

Immunofluorescence assays are described in detail in Supplementary materials and methods.

Dual luciferase reporter assays

Dual luciferase reporter assays are elaborately described in Supplementary materials and methods.

Chromatin immunoprecipitation assays

Cells were fixed and cross-linked with 1% formaldehyde solution for 20 min at room temperature, and cross-linking was terminated with 125 mM glycine. The nuclear material was sheared using a sonicator system (QSONICA).

The chromatin preparation solution was incubated with rotation at 4°C for 1 h with 50 μL of Dynabeads Protein G magnetic beads (Invitrogen) that had been bound with 2-4 μg of the indicated antibodies. Chromatin immune complexes were washed sequentially with low-salt, high-salt, and LiCl buffers. Eluted DNA was purified using the PCR Purification Kit (Thermo Scientific) and analyzed by RT-qPCR using the SYBR Green Master Mix (Bio-Rad). The primer sequences used are presented in Table S1.

In vivo tumorigenicity and metastasis assays

In vivo tumorigenicity and metastasis assays are elaborately described in Supplementary materials and methods.

Statistical analysis

All experiments in this study were independently performed three times under similar conditions. The data were statistically analyzed using IBM SPSS 22.0 and GraphPad Prism 8.0. The relationship between YEATS4 and the clinicopathological characteristics were examined using the χ^2 test. Different groups were compared, and the differences were analyzed using Student's *t* test or one-way ANOVA. The difference in IRS between two groups was analyzed using the Mann-Whitney test. Survival data were analyzed using the Kaplan-Meier method and the log-rank test. The effect of YEATS4 and other clinicopathologic factors on OS and DMFS were evaluated by univariate and multivariate Cox proportional hazard regression analyses. The cBioPortal database was used to analyze the correlation between YEATS4 and core-EMT genes on the basis of the mRNA expression (http://cbioportal.org/) [22]. The *P* value and *R*-value were calculated by cBioPortal. $P < 0.05$ was considered statistically significant.

Results

YEATS4 is highly expressed in breast cancer tumors

A total of 481 patients pathologically diagnosed with primary breast cancer from a retrospective cohort were enrolled in this study. All patients were female with a median age of 52 years (range 22-84 years). The median follow-up time was 123 months. Up to 41.0% of cases were diagnosed with lymph node metastasis during the postoperative pathological examination.

YEATS4 expression in all samples was determined using an antibody previously reported specifically for YEATS4 by immunohistochemistry (IHC) [16]. The reactivity was mainly recognized in the nucleus of breast cancer cells, which was basically in line with previous findings [15]. YEATS4 expression was positive in 325 (67.6%) of the 481 evaluable primary breast cancer tissues, whereas only 15.1% (21/139) of ANTs showed positive immunoreactivity for YEATS4. A significant difference in YEATS4 staining was found between ANTs and breast cancer tissues (**Figure 1A**). The median IRS of YEATS4 staining was markedly higher in breast cancer than in ANTs (**Figure 1B**). Representative images of YEATS4 staining in breast cancer tissues are presented in **Figure 1C**. Of the 481 patients, 68.6% (330) were estrogen receptor (ER)-positive, consisting of 6.1% (20) DCIS and 93.9% (310) IC. Notably, the median YEATS4 staining IRS was markedly higher in the ER-positive group than in the ER-negative group in breast cancer (**Figure 1D**), suggesting that YEATS4 was related to ER expression in breast cancer. The combined data indicate that YEATS4 expression was higher in breast cancer, particularly in the ER-positive group.

YEATS4 expression is correlated with clinicopathologic features

Correlations between YEATS4 expression and clinicopathological parameters in breast cancer were analyzed (**Table 1**). YEATS4 positive expression correlated with pathologically large tumor size ($\chi^2 = 8.107$, $P = 0.017$), ER expression ($\chi^2 = 5.356$, $P = 0.021$), lymph node metastasis ($\chi^2 = 6.520$, $P = 0.011$), and advanced TNM stage ($\chi^2 = 10.566$, $P = 0.005$). For the molecular subtype, 73.6% (67/91) of breast cancer tissues showed positive YEATS4 expression in the Luminal A subtype, 69.9% (186/266) in the Luminal B subtype, 59.0% (46/78) in the HER2 type, and 56.5% (26/46) in the triple-negative breast cancer subtype. However, no significant difference in YEATS4 expression was found among several molecular subtypes of breast cancer ($\chi^2 = 7.388$, $P = 0.061$). YEATS4 expression showed no significant association with other clinicopathologic features, such as age at diagnosis, menopaus-

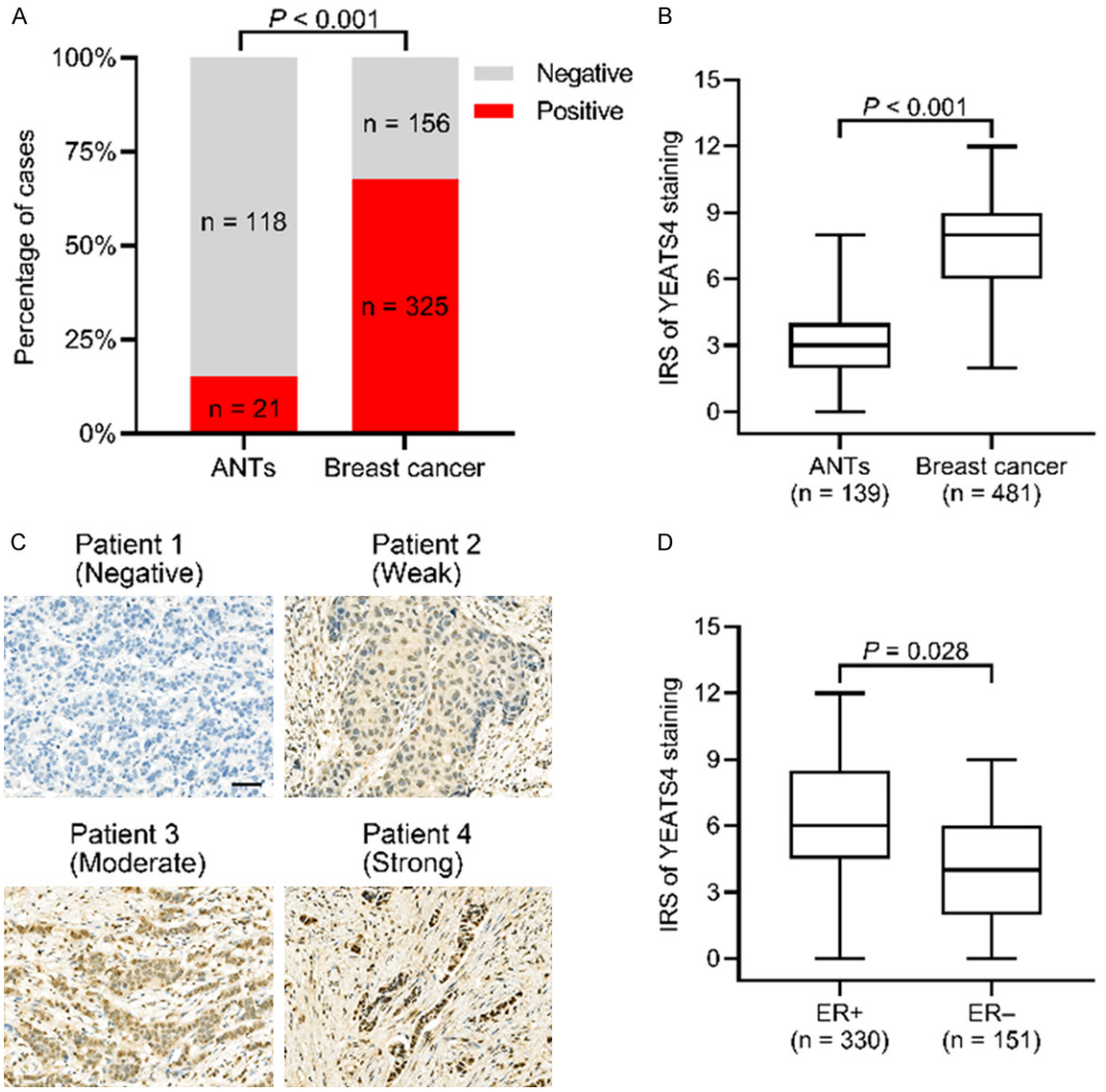

Figure 1. YEATS4 is positively expressed in breast cancer. A. Proportion of positive YEATS4 expression in breast cancer tissues compared with that of adjacent normal tissues (ANTs) ($P < 0.001$). B. Median immunoreactive score (IRS) of YEATS4 staining in breast cancer tissues, which is significantly higher than that in ANTs ($P < 0.001$). C. Representative immunohistochemistry (IHC) imaging of different YEATS4 staining intensities in breast cancer tissues. Scale bar, 50 μm. D. Median IRS of YEATS4 staining being higher in ER-positive than ER-negative breast cancer tissues ($P = 0.028$).

al status, histologic grade, PR and HER2 expression, Ki-67 status, and P53 status. To summarize, positive YEATS4 expression was markedly related to pathologic tumor size, ER expression, lymph node involvement, and TNM staging.

YEATS4 expression is related to breast cancer progression

We examined the YEATS4 expression levels in ANTs (n = 139), DCIS (n = 42), invasive cancer with no lymph node metastasis (ICW, n = 242), and invasive cancer with lymph node metastasis (ICLNM, n = 197). YEATS4 expression was found in 15.1% of ANTs, 47.6% of DCIS, 65.7% of ICW, and 74.1% of ICLNM specimens. Positive YEATS4 expression gradually increased with cancer progression; however, no significant difference was determined between ICW and ICLNM ($P = 0.057$; **Figure 2A**). All subtypes in cancer progression showed increased YEATS4 expression relative to that of ANTs (**Figure 2A**). The IRSs of the ANTs, DCIS, ICW,

Table 1. Association between baseline characteristics and YEATS4 expression

Clinicopathological criteria	Expression of YEATS4			χ^2	*P*-value
	Positive (n = 325)	Negative (n = 156)	Total (n = 481)		
Age at diagnosis (years)					
≤ 35	59 (74.7%)	20 (25.3%)	79	2.184	0.139
> 35	266 (66.2%)	136 (33.8%)	402		
Pathologic tumor size (cm)					
T1	93 (59.2%)	64 (40.8%)	157	8.107	**0.017**
T2	201 (70.8%)	83 (29.2%)	284		
T3	31 (77.5%)	9 (22.5%)	40		
Menopausal status					
Premenopausal	138 (65.7%)	72 (34.3%)	210	0.584	0.445
Postmenopausal	187 (69.0%)	84 (31.0%)	271		
Histological grade					
1	50 (75.8%)	16 (24.2%)	66	4.426	0.219
2	135 (63.4%)	78 (36.6%)	213		
3	114 (70.4%)	48 (29.6%)	162		
Unknown	26 (65.0%)	14 (35.0%)	40		
ER					
Positive	234 (70.9%)	96 (29.1%)	330	5.356	**0.021**
Negative	91 (60.3%)	60 (39.7%)	151		
PR					
Positive	206 (64.2%)	105 (35.8%)	311	0.710	0.400
Negative	119 (70.0%)	51 (30.0%)	170		
HER2					
Negative	243 (66.4%)	123 (33.6%)	366	0.963	0.326
Positive	82 (71.3%)	33 (28.7%)	115		
Lymph node metastasis					
Negative	179 (63.0%)	105 (37.0%)	284	6.520	**0.011**
Positive	146 (74.1%)	51 (25.9%)	197		
TNM					
I	50 (56.2%)	39 (43.8%)	89	10.566	**0.005**
II	215 (67.8%)	102 (32.2%)	317		
III	60 (80.0%)	15 (20.0%)	75		
Ki-67 status					
≤ 20%	102 (61.8%)	63 (38.2%)	165	3.789	0.052
> 20%	223 (70.6%)	93 (29.4%)	316		
P53 status					
Positive	209 (67.9%)	99 (32.1%)	308	0.944	0.624
Negative	100 (65.8%)	52 (34.2%)	152		
Unknown	16 (76.2%)	5 (23.8%)	21		
Molecular subtype					
Luminal A	67 (73.6%)	24 (26.4%)	91	7.388	0.061
Luminal B	186 (69.9%)	80 (30.1%)	266		
HER2 type	46 (59.0%)	32 (41.0%)	78		
TNBC	26 (56.5%)	20 (43.5%)	46		

YEATS4, YEATS domain-containing protein 4; TNM, tumor-node-metastasis; ER, estrogen receptor; PR, progesterone receptor; HER2, human epidermal growth factor receptor 2; TNBC, triple-negative breast cancer. *P*-values that reach significance are in bold.

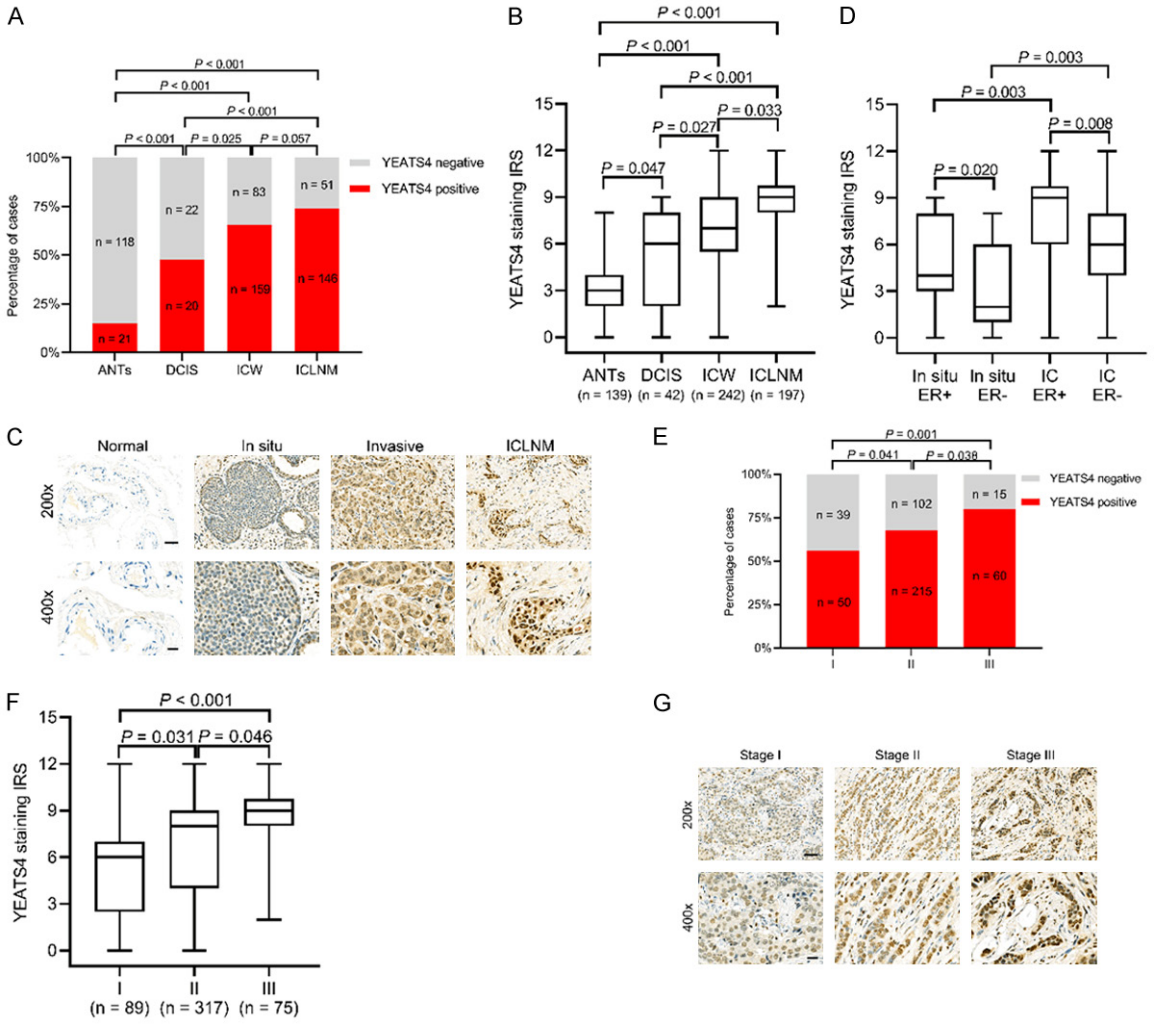

Figure 2. YEATS4 promotes the progression of breast cancer. A. Percentage of positive YEATS4 expression in adjacent normal tissues (ANTs), ductal carcinoma *in situ* (DCIS), invasive carcinoma without lymph node metastasis (ICW), and invasive carcinoma with lymph node metastasis (ICLNM). B. Comparison of the median immunoreactive scores (IRSs) of YEATS4 staining among ANTs, DCIS, ICW, and ICLNM specimens. C. Representative images of YEATS4 staining of ANTs, DCIS, ICW, and ICLNM specimens. Scale bar, 50 μm for 200×; 20 μm for 400×. D. Median IRS being higher in invasive carcinoma than in DCIS under the same ER status. E. Percentage of positive YEATS4 expression at different TNM stages. F. Comparison of median IRS of YEATS4 staining among stages I, II, and III. G. Representative YEATS4 images at stages I, II, and III. Scale bar, 50 μm for 200×; 20 μm for 400×.

and ICLNM specimens were gradually increased, and significant differences among the groups were found (**Figure 2B**). Representative images of the YEATS4 staining of ANTs, DCIS, ICW, and ICLNM specimens are presented in **Figure 2C**. The YEATS4 expression of the IC subtype was higher than that of the DCIS subgroup independent of ER expression, whereas IRS was increased in both the IC subtype and the DCIS subgroup with ER-positive expression (**Figure 2D**). The finding further supports that YEATS4 expression was correlated with ER expression.

We then explored the relationship between YEATS4 expression and TNM stage. The positive rate of YEATS4 in stage I was 56.2%, which increased to 67.8% and 80.0% in stages II and III, respectively (**Figure 2E**). Significant differences in YEATS4 IRS were indicated among the subgroups based on the TNM stage (**Figure 2F**). Representative photomicrographs of the YEATS4 immunohistochemical staining of each TNM stage are presented in **Figure 2G**. Overall, YEATS4 expression is correlated with progression in breast cancer and can potentially play a critical role in cancer development.

YEATS4 expression is correlated with poor prognosis in breast cancer

The effect of YEATS4 expression on clinical survival in patients with breast cancer was examined using the Kaplan-Meier method. Within the follow-up period, 62 (12.8%) patients died-49 (15.1%) from the YEATS4-positive group with 325 cases and 13 (8.3%) from the YEATS4-negative group with 156 cases. The 10-year OS was 84.0% in the YEATS4-negative group, and 67.4% in the YEATS4-positive group (univariate Cox regression HR 2.270, 95% CI 1.397-3.691, P = 0.001; **Figure 3A**; **Table 2**). Multivariate analysis indicated that positive YEATS4 expression was an independent poor prognostic indicator for OS (HR 1.969, 95% CI 1.146-3.382, P = 0.013; **Table 2**).

Distant metastasis occurred in 93 patients during the follow-up period-77 (23.4%) from the YEATS4-positive group with 325 cases and 16 (10.3%) from the YEATS4-negative group with 156 cases. The 10-year DMFS was 77.8% in the YEATS4-negative group and 56.1% in the YEATS4-positive group (univariate Cox regression HR 1.892, 95% CI 1.137-3.188, P = 0.015; **Figure 3B**; **Table 3**). When all eligible prognostic variables were subjected to multivariate Cox regression analysis, coupled with lymph node metastasis, positive YEATS4 expression was considered as an independent indicator for DMFS (HR 1.784, 95% CI 1.016-3.002, P = 0.029; **Table 3**).

The influence of YEATS4 expression on OS was further stratified by the TNM stage and the molecular subtypes to better identify patients who were at high risk. YEATS4 expression was negatively related to OS in stage II and III groups (P = 0.044, P = 0.043, respectively), instead of the stage I group (P = 0.218) (**Figure 3C**, **3E**), indicating that positive YEATS4 expression could be a potential index for poor clinical outcome in patients with breast cancer. In addition, in the subgroup analyses based on molecular subtype (**Figure 3F-I**), YEATS4 expression was correlated with shortened OS in the subtype of Luminal B (P = 0.019), HER2 (P = 0.037), and TNBC (P = 0.012), but not Luminal A (P = 0.333).

We then explored the association between YEATS4 expression and DMFS in the ICLNM subgroup (**Figure 3J**). ICLNM with positive YEATS4 expression showed a high incidence of distant metastasis (P = 0.015). These results indicated that YEATS4 expression is an independent poor prognostic indicator for DMFS, particularly in ICLNM.

YEATS4 promotes the proliferation of breast cancer cells in vitro and in vivo

The aforementioned results indicated that positive YEATS4 expression was related to disease progression in patients with breast cancer. Therefore, we determined whether YEATS4 was involved in tumor growth. We established YEATS4-deleting MDA-MB-231 and SK-BR-3 cells (named as MDA-MB-231-shYEATS4 and SK-BR-3-shYEATS4) and YEATS4-overexpressing T-47D and ZR-75-1 cells (designated as T-47D-YEATS4 and ZR-75-1-YEATS4) by lentivirus infection. YEATS4 expression was verified by RT-qPCR and Western blot analysis (**Figure 4A**, **4B**). The proliferation rate was significantly reduced in shYEATS4 breast cancer cells (**Figure 4C**). Plate colony formation assay and soft agar colony formation assay indicated that compared with control cells, MDA-MB-231-shYEATS4 and SK-BR-3-shYEATS4 cells formed fewer colonies (**Figure 4D**, **4E**). Increased YEATS4 expression also markedly promoted the proliferation of T-47D and ZR-75-1 cells (**Figure 4F**). The colony-forming ability of T-47D -YEATS4 and ZR-75-1-YEATS4 cells in the regular plate or the soft agar was evidently improved (**Figure 4G**, **4H**). We continued to evaluate the effect of YEATS4 on tumorigenicity in subcutaneous xenograft nude mice models. YEATS4 depletion evidently reduced the volume and weight of xenograft tumors (**Figure 4I-K**), whereas YEATS4 overexpression significantly promoted tumor growth (**Figure 4L-N**). The aforementioned findings suggested that YEATS4 played an important role to promote the growth of breast cancer cells *in vitro* and *in vivo*.

YEATS4 promotes the migration and invasion of cancer cells in vitro and in vivo

YEATS4 was closely related to distant metastasis in patients with breast cancer, prompting the investigation of the function of YEATS4 in cancer metastasis. YEATS4 expression in normal breast epithelial cells and several breast

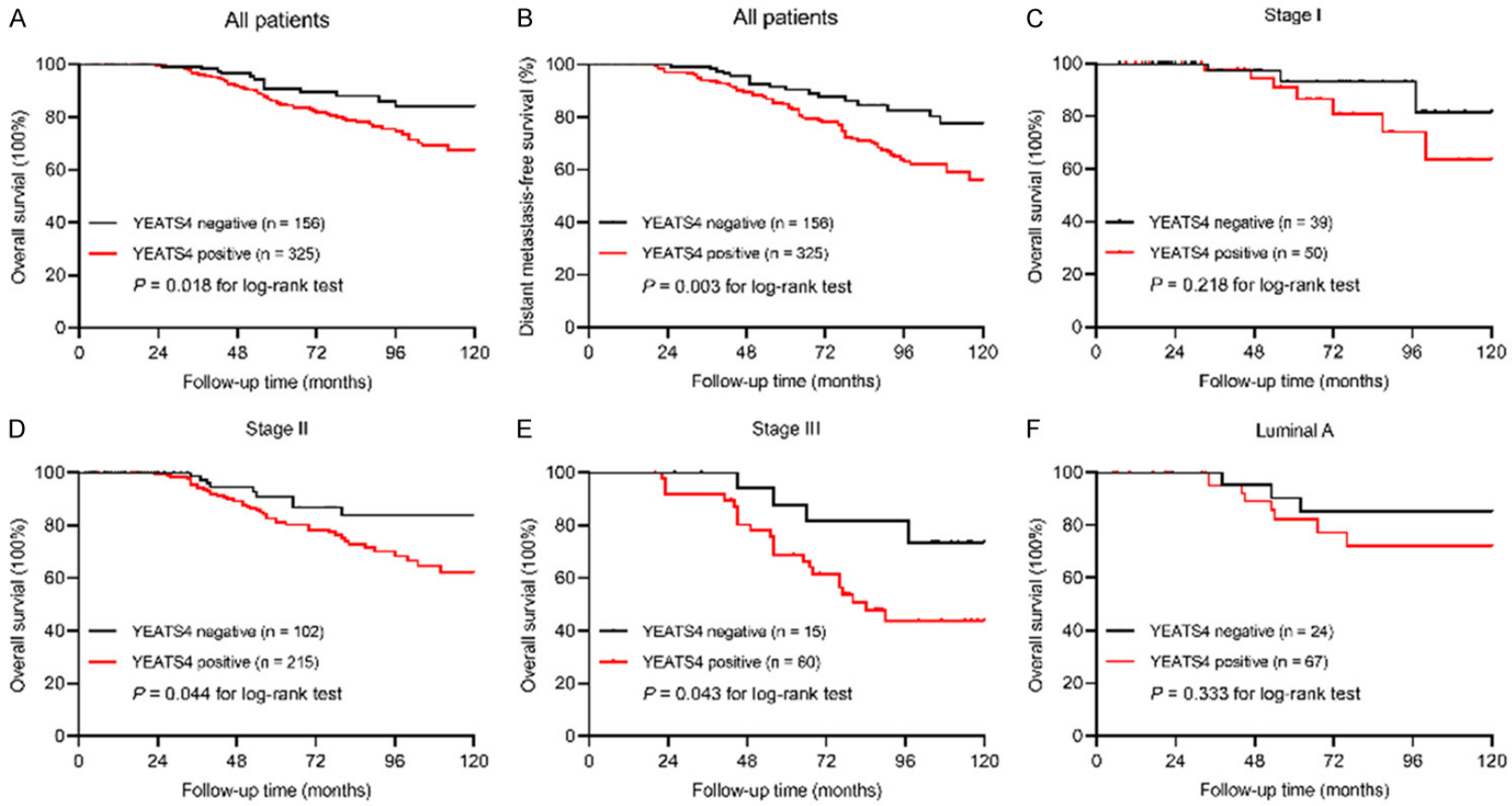
A
All patients
Overall survial (100%)
YEATS4 negative (n = 156)
YEATS4 positive (n = 325)
P = 0.018 for log-rank test
Follow-up time (months)
B
All patients
Distant metastasis-free survival (%)
YEATS4 negative (n = 156)
YEATS4 positive (n = 325)
P = 0.003 for log-rank test
Follow-up time (months)
C
Stage I
Overall survial (100%)
YEATS4 negative (n = 39)
YEATS4 positive (n = 50)
P = 0.218 for log-rank test
Follow-up time (months)
D
Stage II
Overall survial (100%)
YEATS4 negative (n = 102)
YEATS4 positive (n = 215)
P = 0.044 for log-rank test
Follow-up time (months)
E
Stage III
Overall survial (100%)
YEATS4 negative (n = 15)
YEATS4 positive (n = 60)
P = 0.043 for log-rank test
Follow-up time (months)
F
Luminal A
Overall survial (100%)
YEATS4 negative (n = 24)
YEATS4 positive (n = 67)
P = 0.333 for log-rank test
Follow-up time (months)

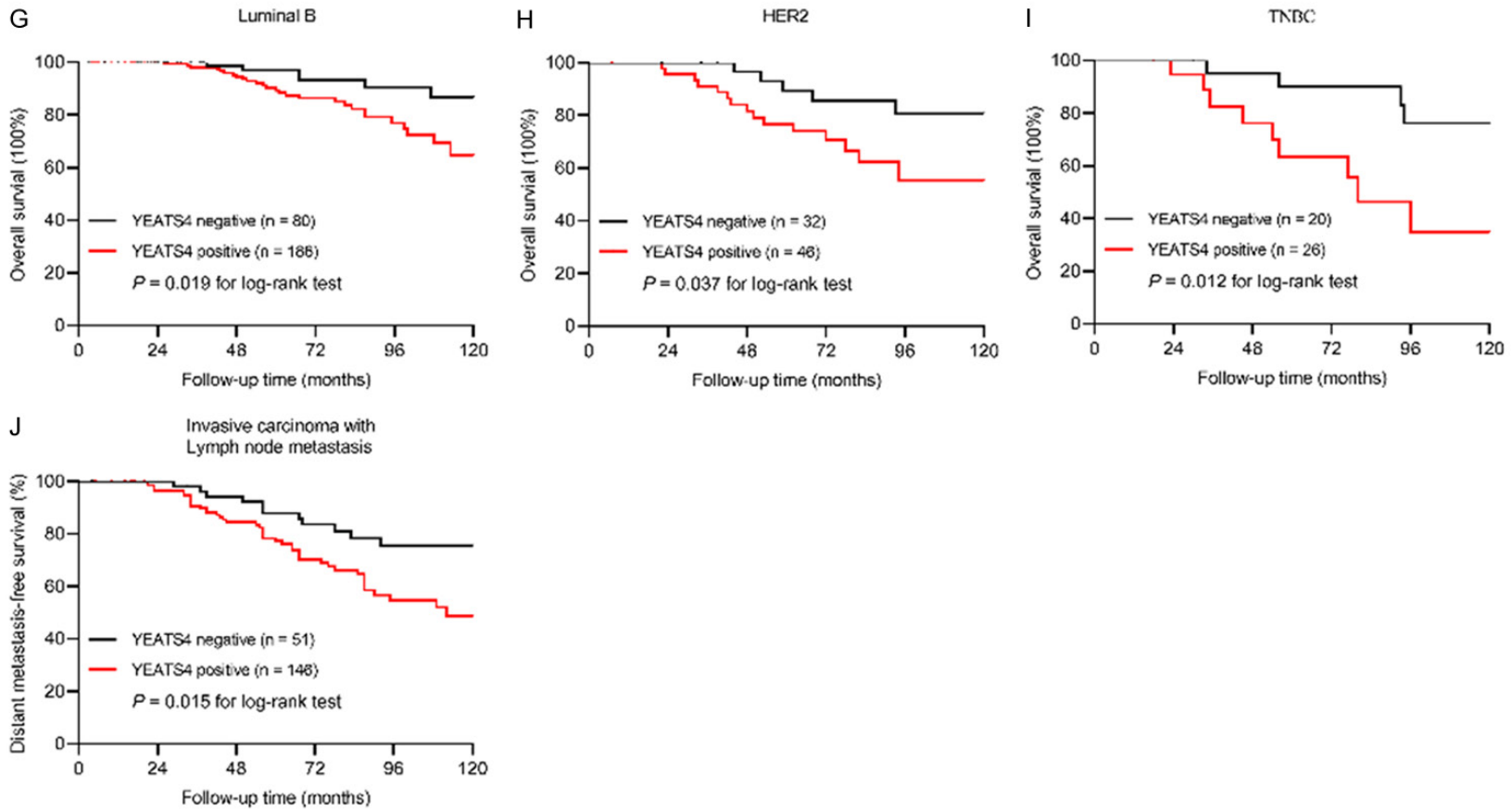

Figure 3. YEATS4 has a prognostic value in breast cancer. A, B. Kaplan-Meier curves for the correlation between YEATS4 expression and overall survival (OS, P = 0.018) or distant metastasis-free survival (DMFS, P = 0.003). C-E. OS rate of patients with breast cancer according to different TNM stages. F-I. OS rate of patients with breast cancer, determined based on molecular subtype. J. Correlation of positive YEATS4 expression with a high risk of distant metastasis in invasive carcinoma with lymph node metastasis (P = 0.015).

Table 2. Univariate and multivariate analyses of overall survival in breast cancer patients

Variables	Category	Univariate			Multivariate		
		HR	95% CI	*P*-value	HR	95% CI	*P*-value
Age (Years)	> 35 vs. ≤ 35	0.631	0.388-1.027	0.063	1.080	0.245-4.749	0.918
Tumor size	T2, T3 vs. T1	1.055	0.732-1.520	0.770			
Histological grade	Grade 3 vs. grade 1, 2	1.826	1.068-3.111	**0.027**	1.015	0.676-1.524	0.947
ER	Negative vs. positive	1.765	1.028-4.536	**0.041**	2.472	1.126-4.614	**0.020**
PR	Negative vs. positive	0.405	0.629-2.541	0.329			
HER2	Positive vs. negative	1.280	0.854-1.919	0.230			
Lymph node metastasis	Positive vs. negative	8.157	3.542-17.034	**< 0.001**	5.873	2.906-11.840	**< 0.001**
TNM stage	III vs. I + II	3.392	1.677-6.880	**0.001**	3.325	1.336-8.250	**0.011**
Ki-67 status	> 20% vs. ≤ 20%	1.193	0.990-1.438	0.062	1.110	0.643-1.913	0.705
P53 status	Positive vs. negative	0.742	0.437-1.258	0.268			
YEATS4	Positive vs. negative	2.270	1.397-3.691	**0.001**	1.969	1.146-3.382	**0.013**

ER, estrogen receptor; PR, progesterone receptor; HER2, human epidermal growth factor receptor 2; TNM, tumor-node-metastasis; YEATS4, YEATS domain-containing protein 4. *P*-values that reach significance are in bold.

Table 3. Univariate and multivariate analyses of distant metastasis-free survival in breast cancer patients

Variables	Category	Univariate			Multivariate		
		HR	95% CI	*P*-value	HR	95% CI	*P*-value
Age (Years)	> 35 vs. ≤ 35	0.972	0.389-2.434	0.952			
Tumor size	T2, T3 vs. T1	1.954	0.936-4.083	0.075	1.005	0.634-1.960	0.725
Histological grade	Grade 3 vs. grade 1, 2	1.270	0.518-3.132	0.607			
ER	Negative vs. positive	1.775	1.079-2.941	**0.025**	1.443	0.862-2.387	0.166
PR	Negative vs. positive	1.806	1.194-3.007	**0.007**	1.107	0.589-1.752	0.640
HER2	Positive vs. negative	1.651	0.827-3.304	0.157			
Lymph node metastasis	Positive vs. negative	4.017	2.209-7.303	**< 0.001**	3.543	1.939-6.440	**< 0.001**
TNM stage	III vs. I + II	2.521	1.146-5.541	**0.021**	2.244	1.018-4.944	0.450
Ki-67 status	> 20% vs. ≤ 20%	1.277	0.736-2.213	0.385			
P53 status	Positive vs. negative	0.714	0.165-3.014	0.656			
YEATS4	Positive vs. negative	1.892	1.137-3.188	**0.015**	1.784	1.061-3.002	**0.029**

ER, estrogen receptor; PR, progesterone receptor; HER2, human epidermal growth factor receptor 2; TNM, tumor-node-metastasis; YEATS4, YEATS domain-containing protein 4. *P*-values that reach significance are in bold.

cancer cell lines was evaluated. YEATS4 was highly expressed in MDA-MB-231, MCF-7, MDA-MB-436, and SK-BR-3 cells but poorly expressed in ZR-75-1 and T-47D cells (**Figure 5A**). The relative expression of YEATS4 was significantly correlated with the migration ability of the cells (P = 0.006) (**Figure 5B**). Moreover, YEATS4 deletion in MDA-MB-231 cells evidently reduced their migration and invasion abilities in both the transwell assay and wound healing assay (**Figure 5C**, **5D**). By contrast, YEATS4 overexpression in T-47D cells strengthened cell migration and invasion (**Figure 5E**, **5F**). Notably, the recuperation of YEATS4 expression restored the cell invasion ability of YEATS4-deleting MDA-MB-231 cells (**Figure 5G**). To explore the role of YEATS4 in metastasis *in vivo*, SK-BR-3-shYEATS4 or T-47D-YEATS4 cells (with the corresponding control cells) were injected intravenously into the nude lung metastasis mouse models. YEATS4 deletion reduced the incidence of lung metastasis and decreased the number of metastatic lung nodules while prolonging the overall survival time in the SK-BR-3-shYEATS4 group (**Figure 5H-K**). However, YEATS4 overexpression increased the incidence of lung metastasis and the number of metastatic lung nodules while reducing the overall survival time in the T-47D-YEATS4 group (**Figure 5L-O**). Collectively, these results

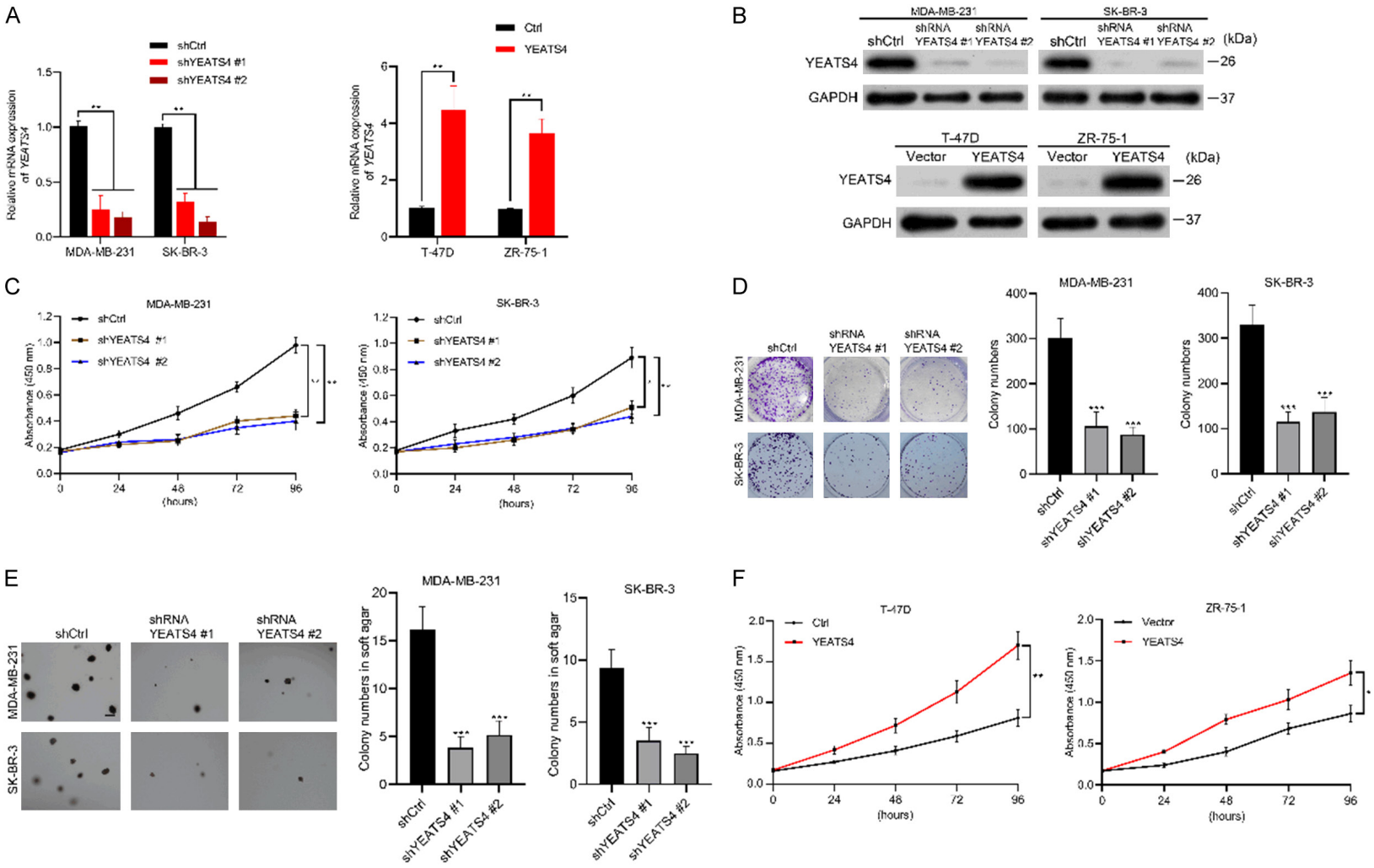
A
shCtrl
shYEATS4 #1
shYEATS4 #2
Relative mRNA expression of YEATS4
MDA-MB-231
SK-BR-3
Ctrl
YEATS4
T-47D
ZR-75-1
B
MDA-MB-231
SK-BR-3
shCtrl
shRNA YEATS4 #1
shRNA YEATS4 #2
(kDa)
YEATS4
GAPDH
T-47D
ZR-75-1
Vector
C
Absorbance (450 nm)
(hours)
D
Colony numbers
E
Colony numbers in soft agar
F
Ctrl
Vector

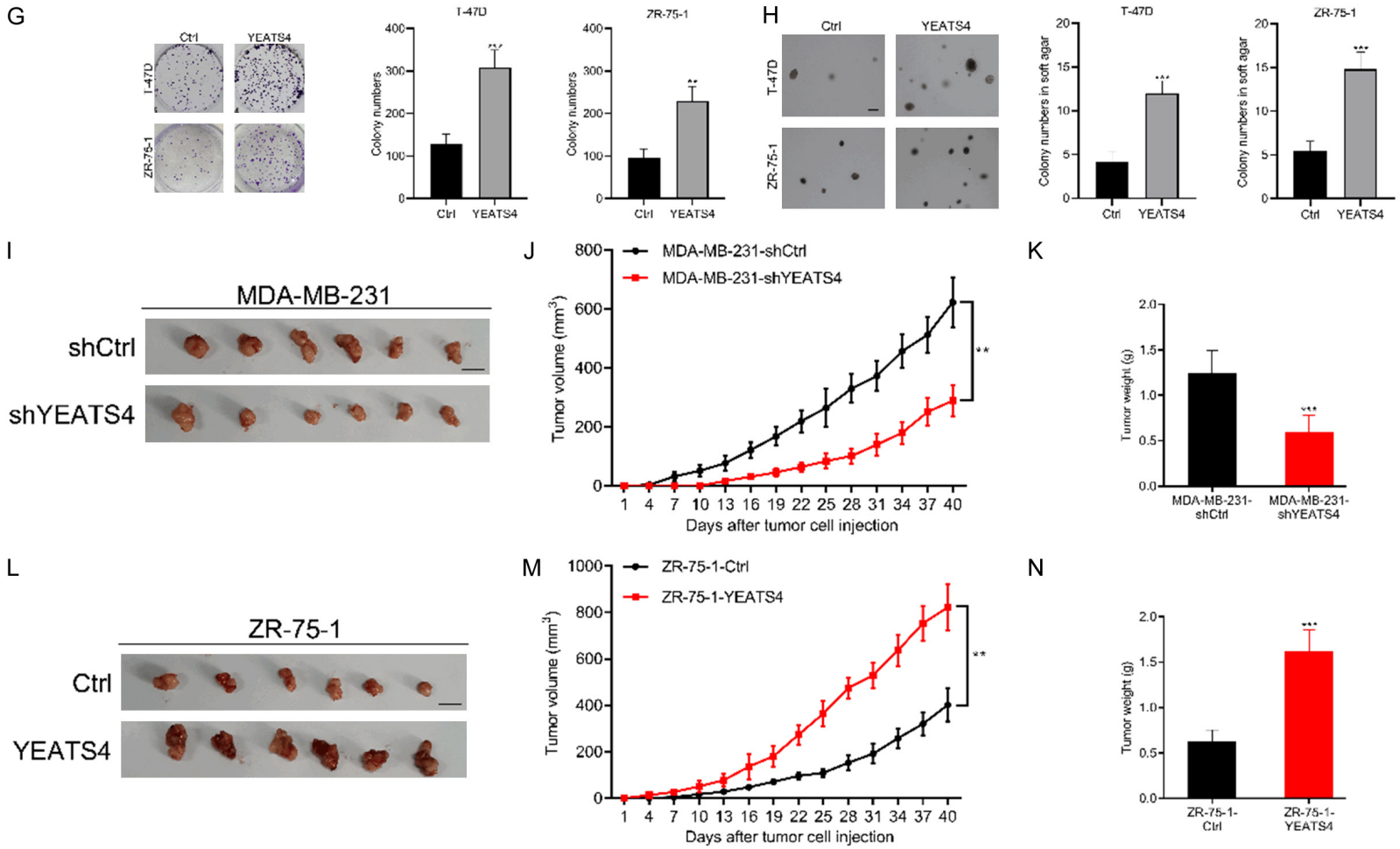

Figure 4. YEATS4 promotes breast cancer cell growth *in vitro* and *in vivo*. (A, B) Verification of the efficiency of YEATS4 deletion by two shRNAs in MDA-MB-231 and SK-BR-3 cells and YEATS4 overexpression in T-47D and ZR-75-1 cells by RT-qPCR (A) and Western blot analysis (B). (C) Influence of YEATS4 deletion on the cell viability of MDA-MB-231 and SK-BR-3 cells, as determined using the CCK-8 assays. (D, E) Effect of YEATS4 knockdown on plate (D) and soft agar (E) colony formation in MDA-MB-231 and SK-BR-3 cells. Scale bar, 200 μm for soft agar colony formation. (F) Effect of YEATS4 overexpression on the cell viability of T-47D and ZR-75-1 cells. (G, H) Influence of YEATS4 overexpression on plate (G) and soft agar (H) colony formation as determined in T-47D and ZR-75-1 cells. Scale bar, 200 μm for soft agar colony formation. (I-K) MDA-MB-231 cells stably transfected with shYEATS4 or shCtrl were subcutaneously injected into the nude mice at a predetermined number of cells (n = 6 for each group). Nude mice were euthanized after 40 d. Representative xenograft tumors in nude mice (I). Scale bar, 1 cm. YEATS4 deletion in MDA-MB-231 cells reduced the volume (J) and weight (K) of tumors. (L-N) ZR-75-1-YEATS4 or control cells were subcutaneously injected into the nude mice (n = 6 for each group). Representative xenograft tumors in the nude mice (L). Scale bar, 1 cm. As shown in (M, N), YEATS4 overexpression in ZR-75-1 cells significantly promoted the tumor growth. Data are presented as mean ± s.d. for 3 independent assays. *, $P < 0.05$; **, $P < 0.01$; ***, $P < 0.001$.

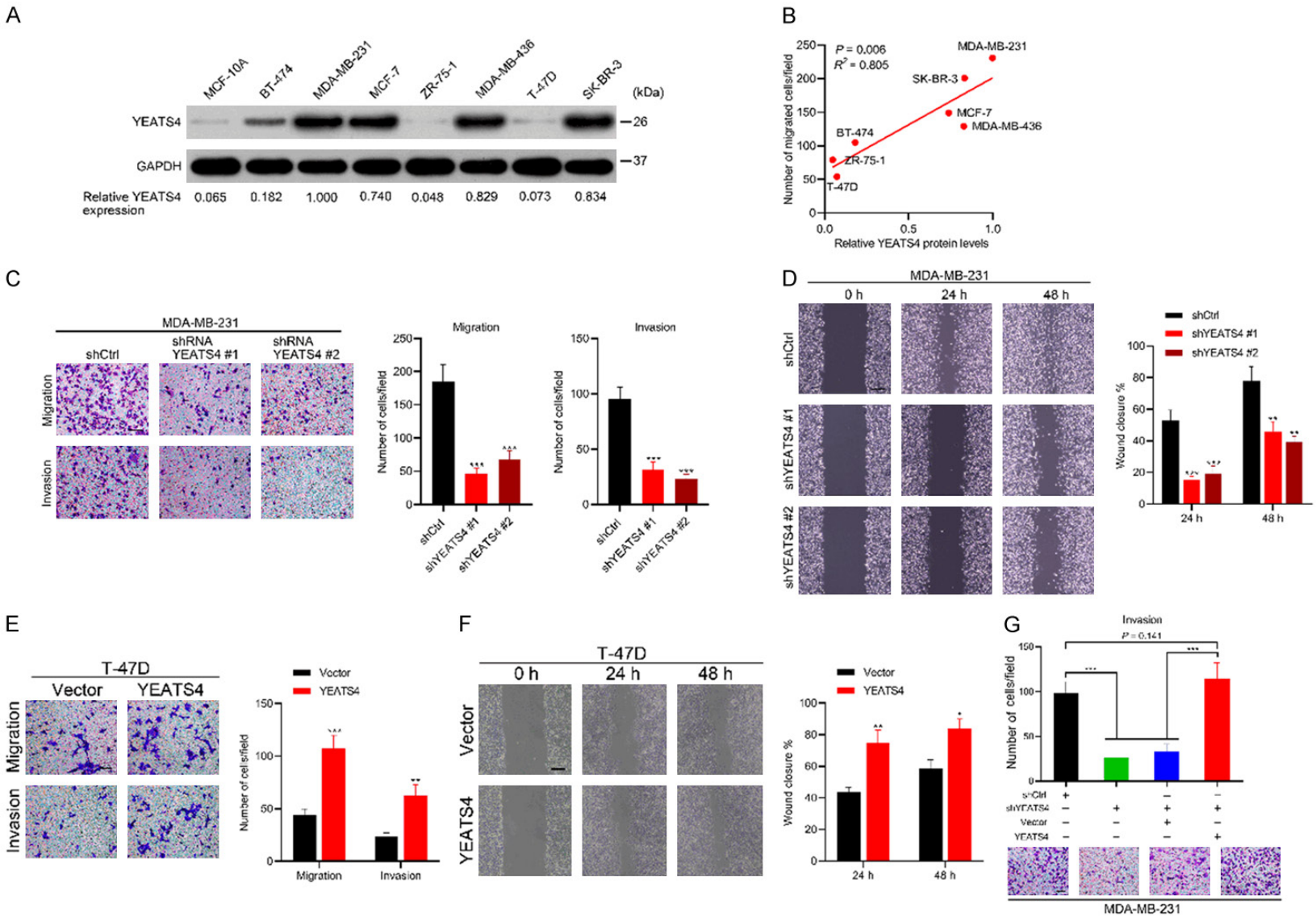
A
MCF-10A
BT-474
MDA-MB-231
MCF-7
ZR-75-1
MDA-MB-436
T-47D
SK-BR-3
(kDa)
YEATS4
26
GAPDH
37
Relative YEATS4 expression
0.065
0.182
1.000
0.740
0.048
0.829
0.073
0.834
B
P = 0.006
R² = 0.805
MDA-MB-231
SK-BR-3
MCF-7
MDA-MB-436
BT-474
ZR-75-1
T-47D
Number of migrated cells/field
Relative YEATS4 protein levels
C
MDA-MB-231
shCtrl
shRNA YEATS4 #1
shRNA YEATS4 #2
Migration
Invasion
Number of cells/field
shCtrl
shYEATS4 #1
shYEATS4 #2
D
MDA-MB-231
0 h
24 h
48 h
shCtrl
shYEATS4 #1
shYEATS4 #2
Wound closure %
E
T-47D
Vector
YEATS4
Migration
Invasion
Number of cells/field
F
T-47D
0 h
24 h
48 h
Vector
YEATS4
Wound closure %
G
Invasion
P = 0.141
Number of cells/field
shCtrl
shYEATS4
Vector
YEATS4
MDA-MB-231

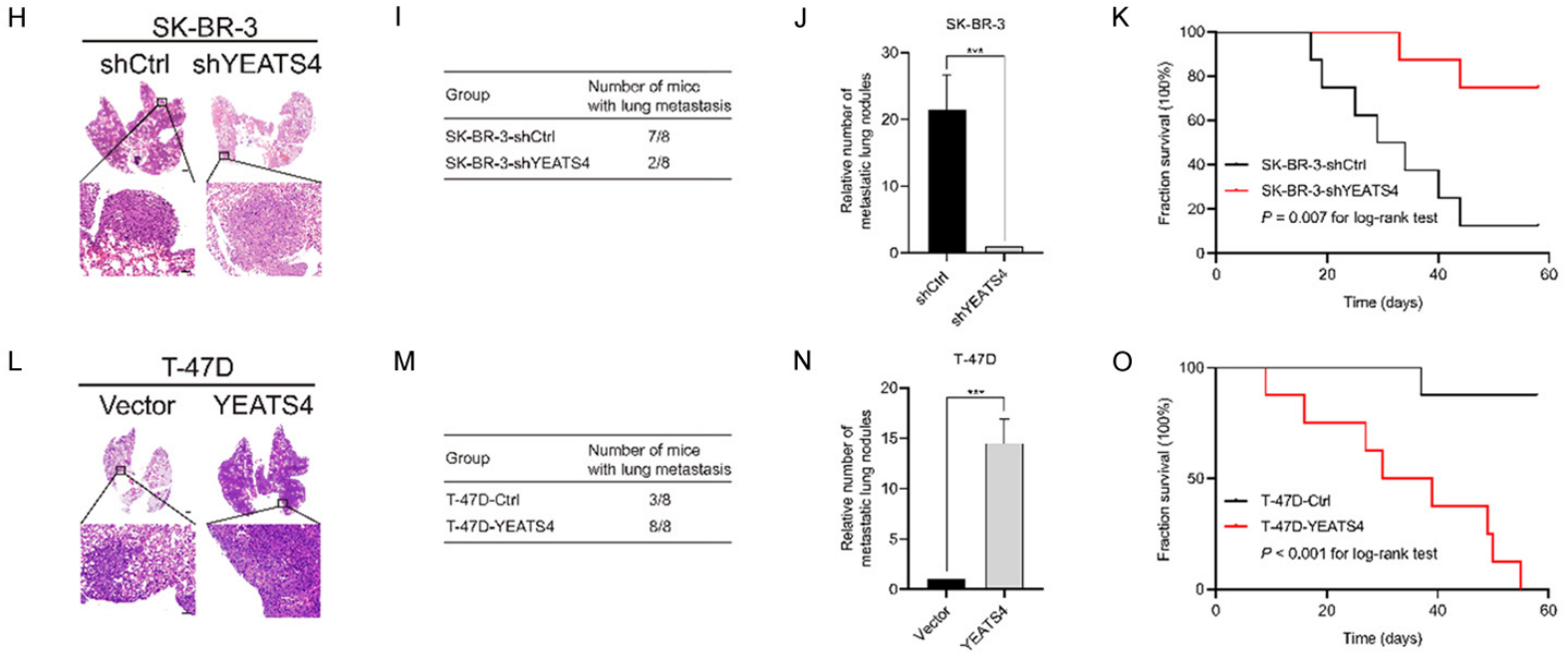

Figure 5. YEATS4 promotes cell migration and invasion in breast cancer cells *in vitro* and in *vivo*. (A) YEATS4 expression detected in several breast cancer cell lines by Western blot analysis. Relative expression of YEATS4 to GAPDH is shown below. (B) Correlation analysis between relative YEATS4 expression and migration ability of cancer cells by using the Pearson correlation method. (C) Migration and invasion capabilities assessed in MDA-MB-231 cells stably infected with lentivirus carrying YEATS4 shRNAs or negative control shRNA (shCtrl) by transwell assays. Scale bar, 50 μm. (D) Migration ability in MDA-MB-231 cells transfected with YEATS4 shRNAs or shCtrl by wound healing assays. Scale bar, 200 μm. (E) Migration and invasion abilities in stable T-47D-YEATS4 cells, determined using transwell assays. Scale bar, 50 μm. (F) Migration capability in stable T-47D-YEATS4 cells, detected by using wound healing assays. Scale bar, 200 μm. (G) YEATS4 was first downregulated by shYEATS4 expressing lentiviruses infection. These cells were then infected with YEATS4 overexpression lentiviruses or control vector overexpression lentiviruses. These different groups of MDA-MB-231 cells were subjected to transwell invasion assays. Scale bar, 50 μm. (H-K) Stable SK-BR-3-shYEATS4 or negative control cells intravenously injected into mice in lung metastasis assays (n = 8 for each group). Representative images of H&E-stained lung tissues from the different groups (H). Scale bar, 1 mm for upper panel and 100 μm for lower panel. Number of nude mice with lung metastasis in each group (I). Relative number of lung metastasis nodules in each group (J). Overall survival time in the different groups of nude mice (K). (L-O) T-47D-YEATS4 or control cells intravenously injected into mice in lung metastasis assays (n = 8 for each group). Representative images of H&E-stained lung tissues from the different groups (L). Scale bar similar to that in (H). Number of nude mice with lung metastasis in each group (M). Relative number of lung metastasis nodules in each group (N). Overall survival time in the different groups of nude mice (O). **, $P < 0.01$; ***, $P < 0.001$.

suggested that YEATS4 promoted the invasion and metastasis of breast cancer cells *in vitro* and *in vivo*.

YEATS4 regulates epithelial-to-mesenchymal transition in breast cancer cells

Growing evidence suggests that EMT is activated during tumor progression and metastasis in response to a deregulated genome [7, 23]. Transcriptomic analyses of YEATS4 in several types of cancer cells indicate that YEATS4 regulates various functional gene groups and pathways, including EMT [24-27]. We first investigated the expression of EMT markers mediated by the differential expression of YEATS4. YEATS4 depletion increased the expression of epithelial markers (E-cadherin and ZO-1) and reduced the expression of mesenchymal markers (vimentin and N-cadherin) in MDA-MB-231 and SK-BR-3 cells (**Figure 6A-C**). By contrast, YEATS4 overexpression decreased the expression of epithelial markers and increased the expression of mesenchymal markers in T-47D and ZR-75-1 cells (**Figure 6D-F**). The findings suggest that YEATS4 is a determinant to promote EMT in breast cancer cells.

YEATS4 transcriptionally regulates ZEB1 expression

EMT is regulated by a complicated network, consisting of EMT transcriptional factors (EMT-TF), namely, TWIST1, SNAIL, SLUG, ZEB families, FOXC2, E47, HMGA2 and epigenetic regulators such as BMI1 and EZH2 [7, 28]. We first integrated and analyzed the RNA sequencing (RNA-seq) data in breast cancer samples from the METABRIC dataset to determine the correlation between the mRNA expression levels of YEATS4 and EMT-TF by using the cBioPortal database [22]. YEATS4 was positively associated with most EMT-TF genes in varying degrees, but ZEB1 was the most relevant gene (Figure S1). Subsequently, we screened the mRNA expression changes of the above EMT regulatory factors in four breast cancer cell lines after stable YEATS4 deletion. Although several genes responded to YEATS4 knockdown, the ZEB1 mRNA expression levels markedly and steadily decreased in all four cell lines (**Figure 7A**). Immunofluorescence experiments indicated a high association between YEATS4 and ZEB1 expression in BT-474 cells (**Figure 7B**), which was further demonstrated by the results that ZEB1 was reduced or elevated with YEATS4 downregulation or overexpression (**Figure 7C**, **7D**). Moreover, YEATS4 restoration in YEATS4-downregulated cells allowed the recovery of ZEB1 expression and maintained a low level of E-cadherin expression (**Figure 7E**). However, ZEB1 deletion did not influence YEATS4 expression (**Figure 7F**). Meanwhile, similar to YEATS4 depletion, ZEB1 deletion exhibited a similar effect on both cell phenotypes and migration capability in the presence of YEATS4, suggesting that ZEB1 is integral for YEATS4-mediated EMT (**Figure 7F**).

We determined whether YEATS4 as a transcription factor mediates ZEB1 via transcription. YEATS4 overexpression plasmids were transiently transfected into ZR-75-1 cells. Consequently, the expression levels of ZEB1 mRNA and protein were elevated (**Figure 7G**, **7H**). In addition, ZEB1 promoter activity was markedly enhanced in 48 h, indicating that the regulatory effect of YEATS4 on ZEB1 expression occurs at the level of transcription (**Figure 7I**). Corresponding to the aforementioned results, YEATS4 increased the ZEB1 promoter activity dose-dependently (**Figure 7J**).

We determined how this modulatory effect is demonstrated at the transcript level. The YEATS domain proteins were recently identified as a group of histone acetyl-lysine readers to influence gene transcription [25, 29, 30]. To explore whether YEATS4 mediates histone modification, acetylated histone modification markers were evaluated by altering the level of YEATS4 expression. Among H3K4, H3K9, H3K14, H4K18, and H3K27, only acetylated-H3K27 (H3K27ac) was influenced by changes in YEATS4 expression. YEATS4 overexpression increased H3K27ac, whereas YEATS4 deletion reduced this modification (**Figure 7K**).

Owing to the correlation of H3K27ac with active transcription [31, 32], we determined whether YEATS4 regulates H3K27ac modification in the ZEB1 promoter. The JASPAR open-access database was used to analyze the occupancy site of the ZEB1 promoter by H3K27ac. The result indicated the presence of three putative-binding sites for histone-occupied abundance (**Figure 7L**). Chromatin immunoprecipitation assay was conducted on T-47D-YEATS4 and MDA-MB-231-shYEATS4 cells. The results

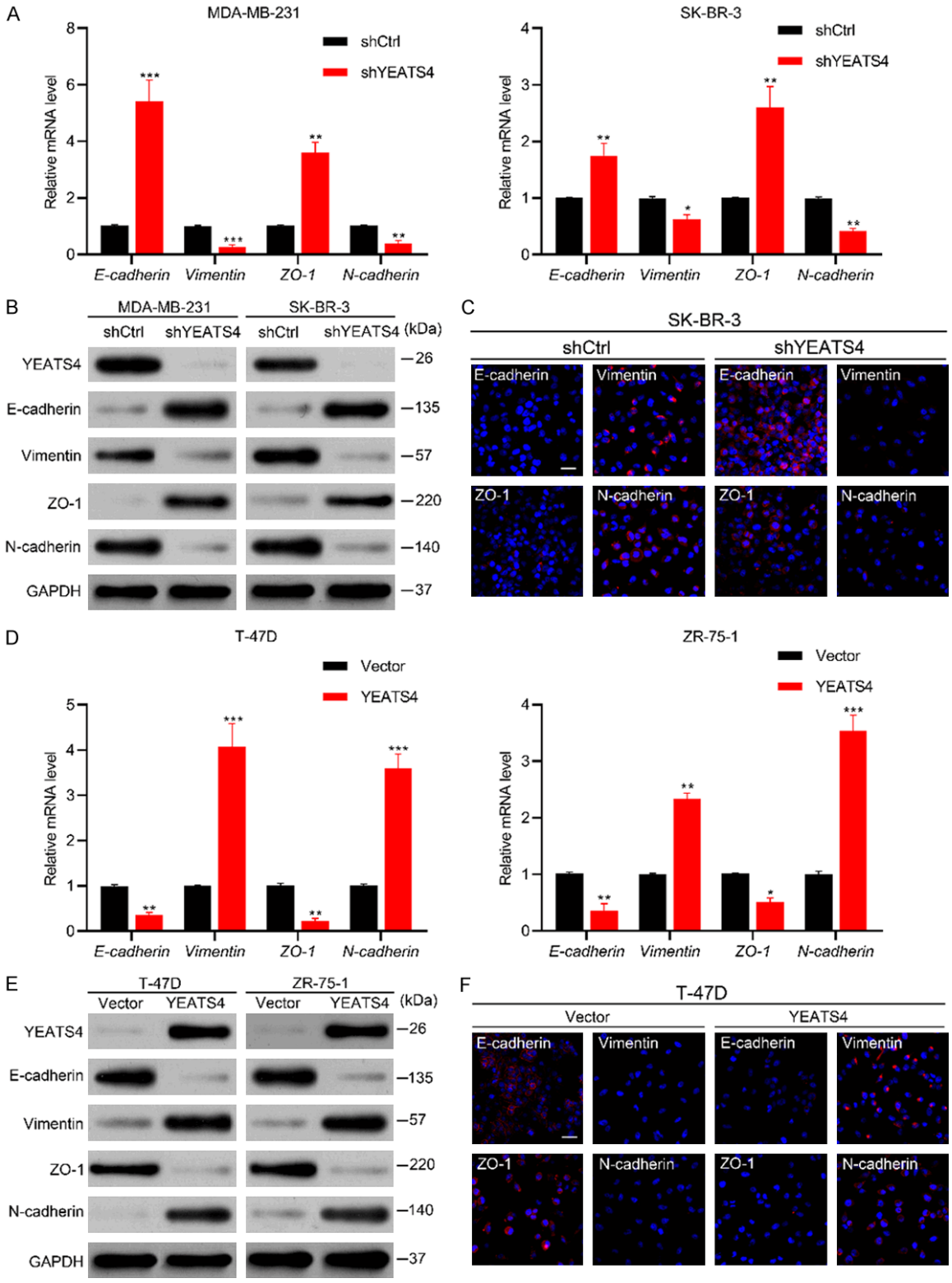

Figure 6. YEATS4 mediates EMT in breast cancer cells. (A) mRNA expression changes in EMT markers, including epithelial markers E-cadherin and ZO-1 and mesenchymal markers vimentin and N-cadherin in MDA-MB-231 and SK-BR-3 cells after stable YEATS4 deletion in RT-qPCR assays. (B) Expression changes in EMT markers were evaluated by Western blot analysis in MDA-MB-231 and SK-BR-3 cells after YEATS4 downregulation. (C) Immunofluorescence images in YEATS4 deleting SK-BR-3 and control cells. Scale bar, 20 μm. (D-F) EMT markers in stable T-47D-YEATS4 and ZR-75-1-YEATS4 cells compared with control cells, as determined by RT-qPCR (D), Western blot analysis (E), and immunofluorescence staining (F; scale bar, 20 μm). Data are presented as mean ± s.d. for 3 independent assays in RT-qPCR. *, $P < 0.05$; **, $P < 0.01$; ***, $P < 0.001$.

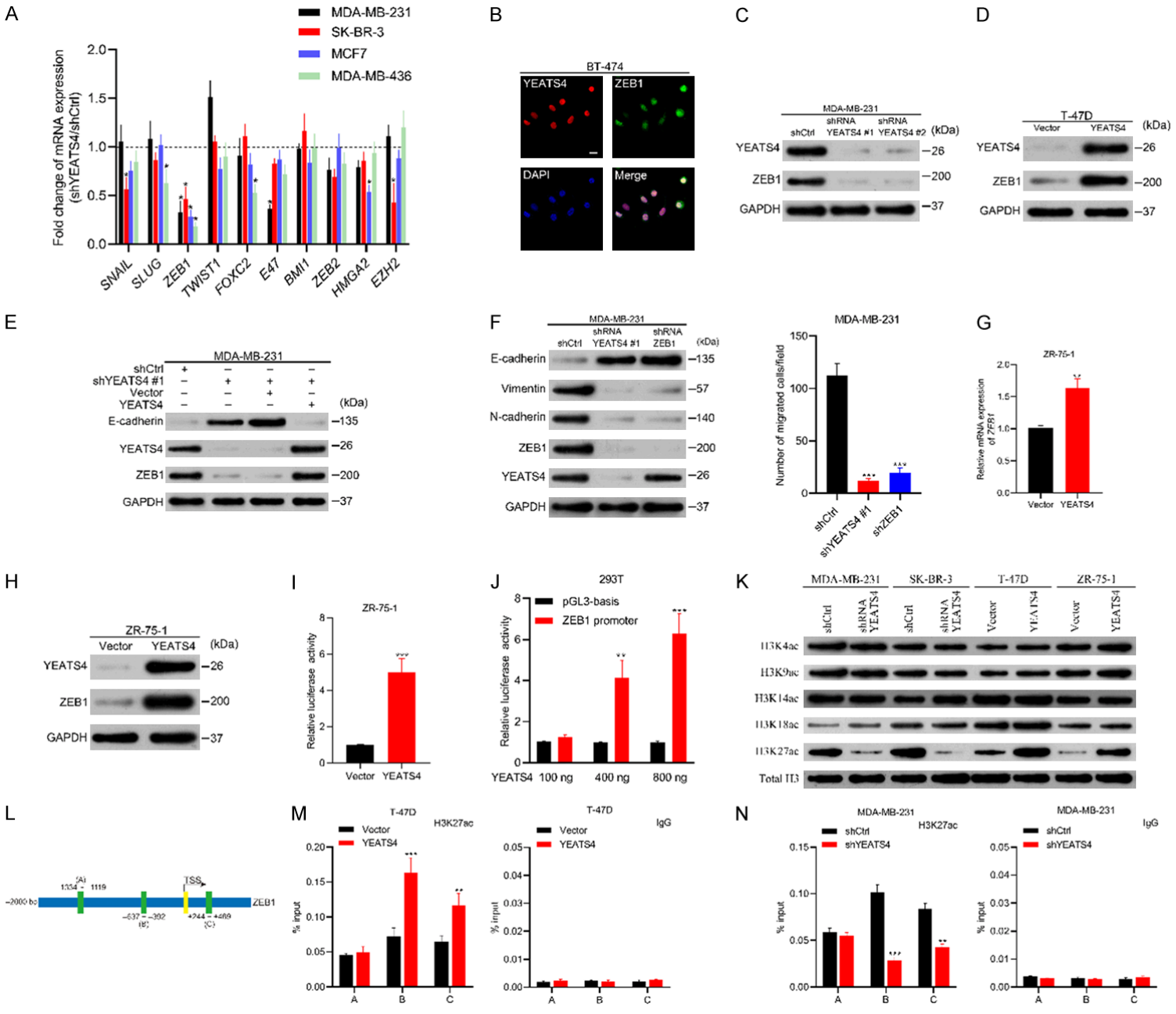
A
MDA-MB-231
SK-BR-3
MCF7
MDA-MB-436
Fold change of mRNA expression (shYEATS4/shCtrl)
SNAIL
SLUG
ZEB1
TWIST1
FOXC2
E47
BMI1
ZEB2
HMGA2
EZH2
B
BT-474
YEATS4
ZEB1
DAPI
Merge
C
MDA-MB-231
shCtrl
shRNA YEATS4 #1
shRNA YEATS4 #2
(kDa)
YEATS4
ZEB1
GAPDH
D
T-47D
Vector
YEATS4
E
MDA-MB-231
shCtrl
shYEATS4 #1
Vector
YEATS4
E-cadherin
F
MDA-MB-231
shRNA ZEB1
Vimentin
N-cadherin
G
ZR-75-1
Relative mRNA expression of ZEB1
H
ZR-75-1
I
Relative luciferase activity
J
293T
pGL3-basis
ZEB1 promoter
YEATS4 100 ng
400 ng
800 ng
K
SK-BR-3
T-47D
ZR-75-1
H3K4ac
H3K9ac
H3K14ac
H3K18ac
H3K27ac
Total H3
L
TSS
ZEB1
M
H3K27ac
IgG
% input
N
shCtrl
shYEATS4

Figure 7. YEATS4 regulates ZEB1 expression transcriptionally. (A) Fold changes in the mRNA expression levels of epithelial-to-mesenchymal transition (EMT) transcriptional factors in four breast cancer cell lines after YEATS4 depletion. Fold changes calculated by normalizing mRNA levels of YEATS4 deletion cells to that of the control cells. (B) Immunofluorescence images of YEATS4 and ZEB1 staining in BT-474 cells. YEATS4 and ZEB1 simultaneously expressed in cancer cells. Scale bar, 20 μm. (C) Expression of YEATS4 and ZEB1 in stable YEATS4-deleting MDA-MB-231 cells, determined by Western blot analysis. (D) YEATS4 and ZEB1 expression in YEATS4-overexpressing T-47D cells, detected by Western blot analysis. (E) Expression changes in ZEB1 and E-cadherin after restoring YEATS4 in YEATS4-deleting MDA-MB-231 cells. (F) Comparison of EMT markers and migration capabilities between YEATS4-deleting or ZEB1-deleting MDA-MB-231 cells and the control group. (G-I) ZEB1 mRNA (G), protein expression levels (H), and promoter activities (I) were investigated after 48 h transient transfection of YEATS4 overexpression or empty vector plasmids in ZR-75-1 cells. (J) Enhancement of the ZEB1 promoter activity by YEATS4 overexpression in a dose-dependent manner. (K) The abundance of H3 lysine acetylation was assessed by Western blot analysis; total H3 was used as a loading control. (L) Schematic of three regions relative to the ZEB1 transcription start site used as primers to test histone-occupied abundance. (M, N) ChIP was conducted to assess H3K27ac occupancy in T-47D-YEATS4 (M) and MDA-MB-231-shYEATS4 (N) cells. IgG was used as a negative control. Percentage of input indicates the ratio of the DNA fragment of each promoter region bound by H3K27ac to the total of the input DNA fragment without the H3K27ac antibody pull-down. Data are presented as mean ± s.d. for 3 independent assays. *, $P < 0.05$; **, $P < 0.01$; ***, $P < 0.001$.

showed that YEATS4 was related to the elevated expression of H3K27ac in the -637 to -392 bp and +244 to +469 bp regions of the ZEB1 promoter in T-47D-YEATS4 cells (**Figure 7M**). The ZEB1 promoter site occupancies by H3K27ac significantly decreased in MDA-MB-231-shYEATS4 cells (**Figure 7N**). However, the occupancies of other acetylated histones such as H3K4, H3K9, H3K14, and H3K18 at the corresponding ZEB1 promoter sites did not change with the variation in YEATS4 expression (Figure S2). The aforementioned findings were consistent with a previous report [25] and suggested that YEATS4 mediated the transcriptional regulation of ZEB1 by modulating H3K27ac and recruiting H3K27ac to the specific sites of the ZEB1 promoter.

ZEB1 is an effector for YEATS4-induced EMT, migration, invasion, and metastasis

We evaluated the role of ZEB1 in the YEATS4-mediated pro-metastatic effect. ZEB1 deletion in T-47D-YEATS4 cells caused the upregulation of epithelial markers and downregulation of mesenchymal markers at the transcriptional (Figure S3) and protein levels (**Figure 8A**). Moreover, ZEB1 knockdown reduced the migration and invasion capabilities of T-47D-YEATS4 cells (**Figure 8B**, **8C**). *In vivo* metastasis assay showed that ZEB1 deletion apparently reduced the incidence of lung metastasis and the number of metastatic lung nodules while increasing the overall survival time in the T-47D-YEATS4 cells (**Figure 8D-G**). These findings indicate that ZEB1 is crucial for YEATS4-mediated breast cancer invasion and metastasis both *in vitro* and *in vivo*.

ZEB1 expression was further examined in our retrospective cohort of human breast cancer patients. ZEB1 expression was detected in 290 (60.3%) of the 481 breast cancer tissues. YEATS4 expression showed a highly positive correlation with ZEB1, as determined by IHC (**Figure 8H**). Similar to that of YEATS4, the positive expression of ZEB1 was gradually increased as the breast cancer progressed (**Figure 8I**, **8J**). To investigate the clinical relevance of the patterns of YEATS4 and ZEB1 expression in human breast cancer, we explored the association between the YEATS4 and ZEB1 expression and DMFS in our cohort. The patients were divided into four groups: $YEATS4^{negative}$-$ZEB1^{negative}$, $YEATS4^{negative}$-$ZEB1^{positive}$, $YEATS4^{positive}$-$ZEB1^{negative}$, and $YEATS4^{positive}$-$ZEB1^{positive}$. DMFS curves were plotted using the Kaplan-Meier method, and differences in survival between groups were compared using the log-rank test (**Figure 8K**). The $YEATS4^{positive}$-$ZEB1^{positive}$ group exhibited a significantly low DMFS. These results are consistent with and verify the aforementioned *in vitro* and *in vivo* findings.

Discussion

The results of this study emphasize the correlation between YEATS4 expression and progression in breast cancer. YEATS4 expression facilitates cell growth, migration, invasion, and EMT *in vitro* and strengthens tumorigenesis and metastasis *in vivo*. By contrast, YEATS4 deletion reverses these malignant phenotypes in otherwise aggressive breast cancer cells. Mechanistically, the results indicate that YEATS4 transcriptionally regulates the expres-

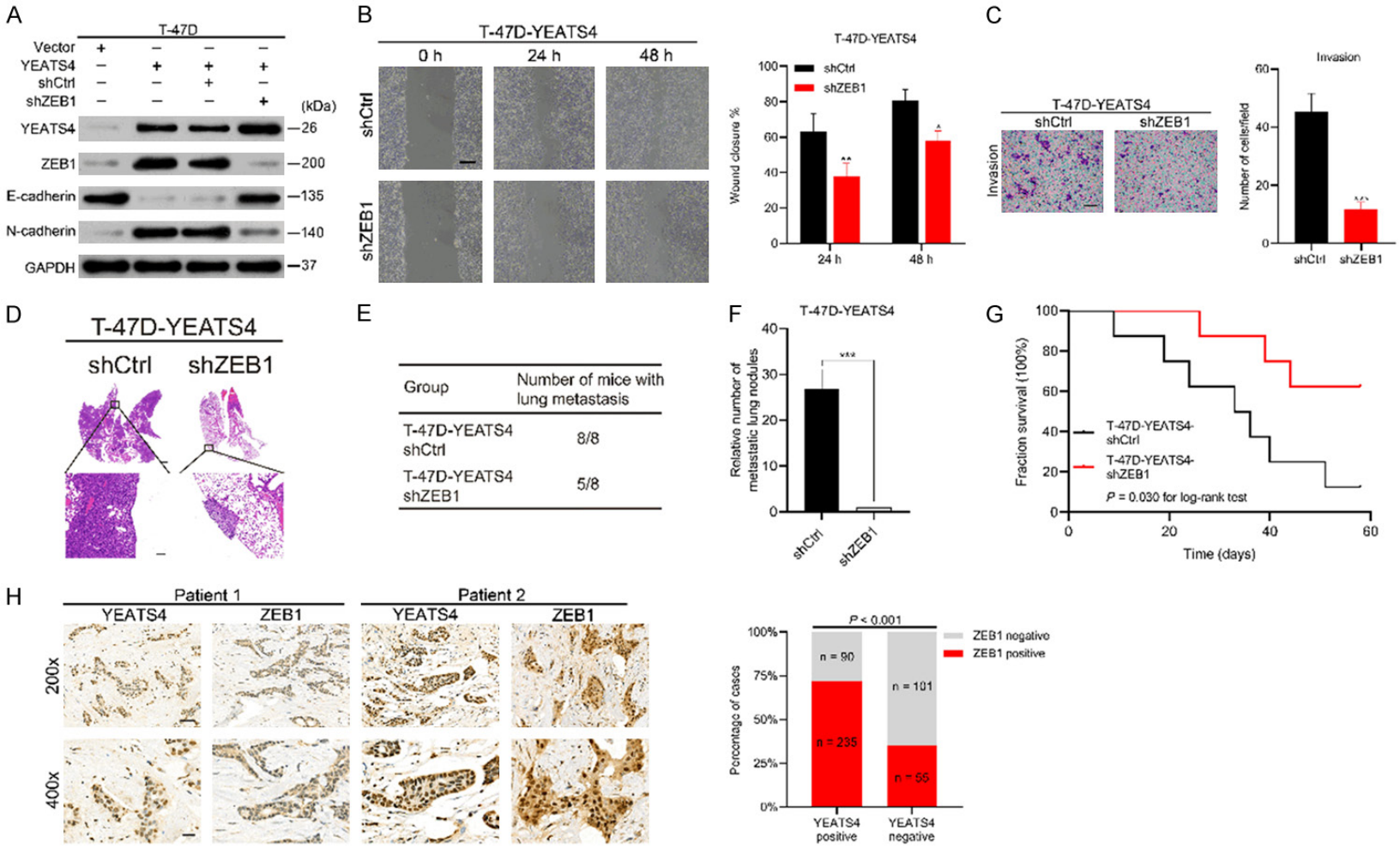
A
T-47D
Vector
YEATS4
shCtrl
shZEB1
(kDa)
YEATS4
ZEB1
E-cadherin
N-cadherin
GAPDH
26
200
135
140
37
B
T-47D-YEATS4
0 h
24 h
48 h
shCtrl
shZEB1
T-47D-YEATS4
shCtrl
shZEB1
Wound closure %
24 h
48 h
C
T-47D-YEATS4
shCtrl
shZEB1
Invasion
Invasion
Number of cells/field
shCtrl
shZEB1
D
T-47D-YEATS4
shCtrl
shZEB1
E
Group
Number of mice with lung metastasis
T-47D-YEATS4 shCtrl
8/8
T-47D-YEATS4 shZEB1
5/8
F
T-47D-YEATS4
Relative number of metastatic lung nodules
shCtrl
shZEB1
G
Fraction survival (100%)
T-47D-YEATS4-shCtrl
T-47D-YEATS4-shZEB1
P = 0.030 for log-rank test
Time (days)
H
Patient 1
Patient 2
YEATS4
ZEB1
YEATS4
ZEB1
200x
400x
P < 0.001
ZEB1 negative
ZEB1 positive
Percentage of cases
n = 90
n = 235
n = 101
n = 55
YEATS4 positive
YEATS4 negative

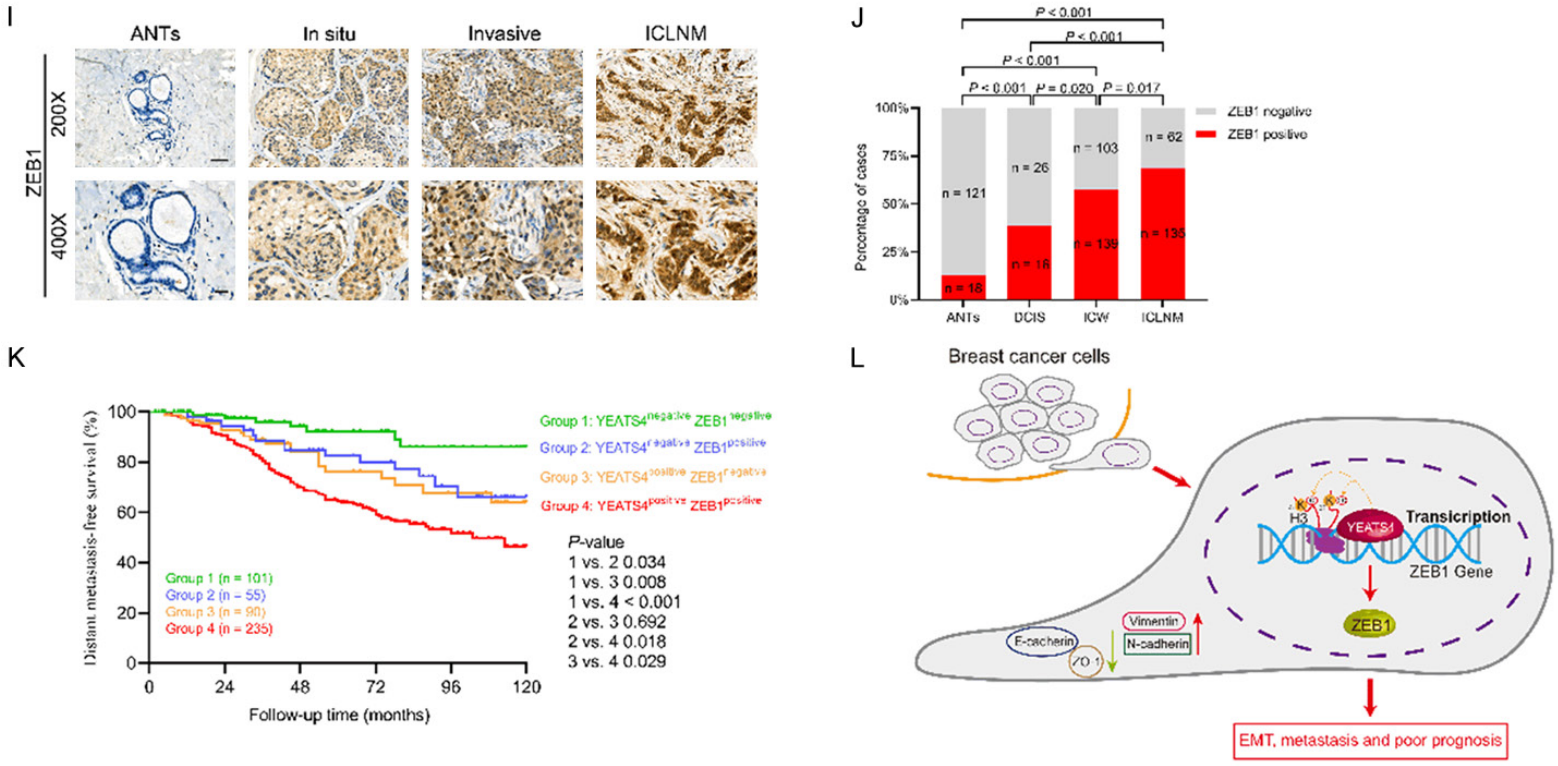

Figure 8. ZEB1 mediates YEATS4-induced EMT and metastasis. (A) Recovery of epithelial marker expression and reduction of mesenchymal marker expression in T-47D-YEATS4 cells by ZEB1 deletion. (B, C) Reduction of YEATS4-induced migration and invasion abilities in T-47D-YEATS4 cells by ZEB1 depletion, as determined by wound healing (B) and transwell invasion (C) assays. Scale bar, 200 μm for (B); 50 μm for (C). (D) Representative images of H&E-stained lung tissues from the T-47D-YEATS4 cells with or without ZEB1 deletion. The scale bars represent 1 mm in upper panel and 100 μm in lower panel. (E) Total number of mice with lung metastasis in different groups. (F) Relative number of lung metastasis nodules in each group. (G) Overall survival of mice in each group. (H) Positive association of YEATS4 expression with ZEB1 expression in breast cancer tissues. Left, representative staining images of YEATS4 and ZEB1. Scale bar, 50 μm for 200×; 20 μm for 400×. (I) Representative images of ZEB1 staining of ANTs, DCIS, ICW, and ICLNM specimens. Scale bar, 50 μm for 200×; 20 μm for 400×. (J) Proportions of ANTs, DCIS, ICW, and ICLNM specimens with ZEB1-positive staining. (K) DMFS curves of patients with breast cancer, plotted based on the expression profiles of YEATS4 and ZEB1 as indicated. Co-expression of YEATS4 and ZEB1 (Group 4) indicating the shortest distant metastasis-free period vs. other groups. (L) Schematic demonstrating the role of YEATS4 in mediating ZEB1 expression, EMT, and metastasis in breast cancer. Data are presented as mean ± s.d. for 3 independent assays. *, $P < 0.05$; **, $P < 0.01$; ***, $P < 0.001$.

sion of the EMT transcription factor ZEB1, which promotes EMT, cancer cell invasion, and metastasis in multiple human cancers [33, 34]. This study reveals a regulatory mechanism by which YEATS4 mediates H3K27ac recruitment at the specific sites of the ZEB1 promoter to facilitate its transcription. ZEB1 deletion weakens the functions of YEATS4 and generates similar results induced by direct YEATS4 deletion. However, direct transactivation or epigenetic modification, which contributes more in YEATS4 transcriptionally regulating ZEB1, requires to be explored further.

Accumulating evidence indicates that YEATS4 is associated with cancer progression in various malignancies [15-17]. In the current study, the IRS of YEATS4 expression gradually increased from ANTs, DCIS, ICW to ICLNM as breast cancer progressed. A gradual increase in the IRS of YEATS4 expression was also observed in TNM stages I, II, and III. These findings suggest that YEATS4 is positively related to the progression of breast carcinoma, which is consistent with previous studies [15-17, 20]. Subgroup analyses showed that the unfavorable effect of positive YEATS4 expression was more significant in stages II and III and luminal B, HER2, and TNBC patients. The reason could be the relatively poor prognosis of patients in these subgroups and the increased occurrence of distant metastasis. Although YEATS4 expression correlated with ER status, YEATS4 seemed to have exerted no effect on OS in luminal A patients. The reason could be that luminal A patients typically showed improved prognosis and reduced recurrence after hormone therapy [35, 36], concealing the effect of YEATS4 expression. A powerful correlation between YEATS4 and shortened survival period was observed in the TNBC subgroup. Owing to the limited choice of treatment for this subgroup [37], YEATS4 concealment could be an effective treatment choice for these patients. In addition, positive YEATS4 expression was related to a significantly low DMFS in patients with ICLNM. These findings suggest that YEATS4 can potentially play an oncogenic role in promoting breast cancer progression and metastasis.

The negative regulatory effect of YEATS4 on multiple well-known tumor suppressors such as p53 and p21 [16, 38], sufficiently proves the feasibility of YEATS4 as an oncogene. Pikor et al. identified YEATS4 as a candidate oncogene by integrative genetic analysis in lung cancer cells and showed that YEATS4 downregulation significantly attenuated cancer cell growth and tumor formation [16]. In the present study, YEATS4 facilitated cell proliferation and strengthened tumorigenicity *in vivo*. YEATS4 could induce EMT and consequently promote metastasis in breast cancer. Breast cancer cells with YEATS4 overexpression represent a mesenchymal phenotype, including relevant enhanced migratory and invasive capabilities *in vitro*. Our findings also indicate that YEATS4 deletion causes MET, suggesting that EMT-MET can be a transforming reciprocal process by manipulating YEATS4 expression. EMT is vital for cancer cells to leave the primary site and form neoplasia in other parts of the body [7]. Malignant phenotypes mediated by YEATS4 overexpression in breast cancer cells result in the aggravation of distant metastases *in vivo*. The results provide a molecular mechanism to explicate the clinical findings that breast cancer patients with positive YEATS4 expression are more likely to succumb to distant metastasis and that YEATS4 is an independent indicator for OS and DMFS.

Our results revealed that ZEB1 is potentially the primary mediator in YEATS4-induced EMT in breast cancer. However, YEATS4 is a multifunctional transcription factor with diverse target genes [10]. The transcriptomic analyses of YEATS4 in several types of cancer cells, including breast cancer cells, demonstrated that YEATS4 regulates various functional gene groups and pathways. In addition to widely-known genes relating to cell cycle, DNA replication, and DNA repair, YEATS4 also regulates some gene groups or pathways that are supposed to be involved in the EMT program, such as gene groups relevant to cell differentiation, cell adhesion, cell locomotory, and extracellular matrix receptor interactions [24-27]. However, transcriptomic data also showed that target genes identified by YEATS4 in different cell models tend to be different and enriched in various functional gene groups [24-26]. Thus, the transcriptional activities of YEATS4 are quite context-dependent. Our results revealed that YEATS4 is mainly involved in promoting ZEB1 transcription and EMT in breast cancer

cells, but the underlying cellular context warrants further study.

The majority of the studies surrounding YEATS4 have focused primarily on cell growth and viability, and few have explored the role of YEATS4 in EMT, migration, and invasion of cancer cells; none of these studies have investigated breast cancer. YEATS4 promoted RNA polymerase II enrichment on the NOTCH2 promoter. Consequently, NOTCH2 expression increased, inducing EMT, migration, and invasion in gastric cancer and hepatocellular cancer [19, 39]. Wild-type p53 forms a ternary complex with MDM2 and Slug to promote the degradation of this EMT inducer [40]. The YEATS4-PP2Cβ complex interacts with and dephosphorylates p53 at serine 366, consequently decreasing p53 stabilization [41]. Thus, YEATS4 can potentially enhance Slug expression. Another study also indicated that YEATS4 deletion by siRNA led to Snail downregulation in pancreatic cancer cells, suggesting the potential role of YEATS4 to mediate EMT [17]. Notably, as a histone acetylation reader, YEATS4 colocalizes with H3K27ac and H3K14ac to promote histone variant H2A.Z deposition onto chromatin to selectively regulate the expression of associated EMT proteins, such as upregulating fibronectin and downregulating E-cadherin in hepatocellular cell carcinoma [25, 42].

The mechanistic link between YEATS4 and ZEB1 was previously unknown. Our results showed that altering the YEATS4 expression changes the acetylation status of H3K27 at the ZEB1 promoter, which subsequently controls ZEB1 expression at the transcription level. However, YEATS4 expression exerted no effect on the acetylation of H3K4, H3K9, H3K14, and H3K18; similarly, no recruitment of these acetylated histones on the ZEB1 promoter was observed. Therefore, YEATS4 transcriptionally regulates ZEB1 expression via the regulation of H3K27 acetylation and enrichment of H3K27ac at specific sites of the ZEB1 promoter. Consequently, YEATS4 promotes EMT, migration, invasion, and metastasis. H3K27ac is identified as an active mark for gene transcription [25, 43]. The YEATS domain of YEATS4 adopts conserved aromatic residues within the "RK" motif to recognize H3K27ac [29]. A recent report suggests that YEATS4 recruits the Dot1l-RNA polymerase II complex onto the target gene promoter by recognizing H3K27ac to initiate transcription [44]. YEATS4 regulation of ZEB1 expression via H3K27ac requires further investigation.

In summary, we demonstrate that YEATS4 expression is increased and significantly associated with the progression of breast cancer. YEATS4 has an oncogenic function in mediating breast cancer EMT and metastasis by transcriptionally regulating ZEB1 expression (**Figure 8L**). The co-upregulation of YEATS4 and ZEB1 is correlated with poor DMFS in our cohort. Our results underscore the critical role of YEATS4 in cancerous signaling. We speculate that YEATS4 is a promising target for therapeutic intervention in breast cancer.

Acknowledgements

This work was supported by the National Natural Science Foundation of China (81670595, 81970568), Shanghai Natural Science Funds (16ZR1428200), and Excellent Youth Medical Talents Program of Shanghai General Hospital (06N1702011).

Disclosure of conflict of interest

None.

Address correspondence to: Drs. Junming Xu and Tao Jin, Department of General Surgery, Shanghai General Hospital, Shanghai Jiao Tong University School of Medicine, 100 Haining Road, Hongkou District, Shanghai 200080, China. Tel: +86-021-63240090 Ext. 3131; Fax: +86-21-63079675; E-mail: junmingxusur@hotmail.com (JMX); Tel: +86-021-63240090 Ext. 3111; Fax: +86-021-6307-9643; E-mail: taojin2198@gmail.com (TJ)

References

[1] Siegel RL, Miller KD and Jemal A. Cancer statistics, 2019. CA Cancer J Clin 2019; 69: 7-34.

[2] Bray F, Ferlay J, Soerjomataram I, Siegel RL, Torre LA and Jemal A. Global cancer statistics 2018: GLOBOCAN estimates of incidence and mortality worldwide for 36 cancers in 185 countries. CA Cancer J Clin 2018; 68: 394-424.

[3] Siegel RL, Jemal A, Wender RC, Gansler T, Ma J and Brawley OW. An assessment of progress in cancer control. CA Cancer J Clin 2018; 68: 329-339.

[4] Demicheli R, Dillekås H, Straume O and Biganzoli E. Distant metastasis dynamics following subsequent surgeries after primary breast cancer removal. Breast Cancer Res 2019; 21: 57.
[5] Weigelt B, Peterse JL and van 't Veer LJ. Breast cancer metastasis: markers and models. Nat Rev Cancer 2005; 5: 591-602.
[6] De Craene B and Berx G. Regulatory networks defining EMT during cancer initiation and progression. Nat Rev Cancer 2013; 13: 97-110.
[7] Pastushenko I and Blanpain C. EMT transition states during tumor progression and metastasis. Trends Cell Biol 2019; 29: 212-226.
[8] Thiery JP. Epithelial-mesenchymal transitions in tumour progression. Nat Rev Cancer 2002; 2: 442-454.
[9] Fischer U, Heckel D, Michel A, Janka M, Hulsebos T and Meese E. Cloning of a novel transcription factor-like gene amplified in human glioma including astrocytoma grade I. Hum Mol Genet 1997; 6: 1817-1822.
[10] Schulze JM, Wang AY and Kobor MS. YEATS domain proteins: a diverse family with many links to chromatin modification and transcription. Biochem Cell Biol 2009; 87: 65-75.
[11] Cai Y, Jin J, Florens L, Swanson SK, Kusch T, Li B, Workman JL, Washburn MP, Conaway RC and Conaway JW. The mammalian YL1 protein is a shared subunit of the TRRAP/TIP60 histone acetyltransferase and SRCAP complexes. J Biol Chem 2005; 280: 13665-13670.
[12] Doyon Y, Selleck W, Lane WS, Tan S and Côté J. Structural and functional conservation of the NuA4 histone acetyltransferase complex from yeast to humans. Mol Cell Biol 2004; 24: 1884-1896.
[13] Wang Y, Jin J, Chung MWH, Feng L, Sun H and Hao Q. Identification of the YEATS domain of GAS41 as a pH-dependent reader of histone succinylation. Proc Natl Acad Sci U S A 2018; 115: 2365-2370.
[14] Tao K, Yang J, Hu Y and Deng A. Knockdown of YEATS4 inhibits colorectal cancer cell proliferation and induces apoptosis. Am J Transl Res 2015; 7: 616-623.
[15] You S, Wang F, Hu Q, Li P, Zhang C, Yu Y, Zhang Y, Li Q, Bao Q, Liu P and Li J. Abnormal expression of YEATS4 associates with poor prognosis and promotes cell proliferation of hepatic carcinoma cell by regulation the TCEA1/DDX3 axis. Am J Cancer Res 2018; 8: 2076-2087.
[16] Pikor LA, Lockwood WW, Thu KL, Vucic EA, Chari R, Gazdar AF, Lam S and Lam WL. YEATS4 is a novel oncogene amplified in non-small cell lung cancer that regulates the p53 pathway. Cancer Res 2013; 73: 7301-7312.
[17] Jixiang C, Shengchun D, Jianguo Q, Zhengfa M, Xin F, Xuqing W, Jianxin Z and Lei C. YEATS4 promotes the tumorigenesis of pancreatic cancer by activating beta-catenin/TCF signaling. Oncotarget 2017; 8: 25200-25210.
[18] Ji S, Zhang Y and Yang B. YEATS domain containing 4 promotes gastric cancer cell proliferation and mediates tumor progression via activating the Wnt/β-catenin signaling pathway. Oncol Res 2017; 25: 1633-1641.
[19] Kiuchi J, Komatsu S, Imamura T, Nishibeppu K, Shoda K, Arita T, Kosuga T, Konishi H, Shiozaki A, Kubota T, Okamoto K, Fujiwara H, Ichikawa D, Tsuda H and Otsuji E. Overexpression of YEATS4 contributes to malignant outcomes in gastric carcinoma. Am J Cancer Res 2018; 8: 2436-2452.
[20] Kim YR, Park MS, Eum KH, Kim J, Lee JW, Bae T, Lee DH and Choi JW. Transcriptome analysis indicates TFEB1 and YEATS4 as regulatory transcription factors for drug resistance of ovarian cancer. Oncotarget 2015; 6: 31030-31038.
[21] Remmele W and Stegner HE. Recommendation for uniform definition of an immunoreactive score (IRS) for immunohistochemical estrogen receptor detection (ER-ICA) in breast cancer tissue. Pathologe 1987; 8: 138-140.
[22] Cerami E, Gao J, Dogrusoz U, Gross BE, Sumer SO, Aksoy BA, Jacobsen A, Byrne CJ, Heuer ML, Larsson E, Antipin Y, Reva B, Goldberg AP, Sander C and Schultz N. The cBio cancer genomics portal: an open platform for exploring multidimensional cancer genomics data. Cancer Discov 2012; 2: 401-404.
[23] Pastushenko I, Brisebarre A, Sifrim A, Fioramonti M, Revenco T, Boumahdi S, Van Keymeulen A, Brown D, Moers V, Lemaire S, De Clercq S, Minguijón E, Balsat C, Sokolow Y, Dubois C, De Cock F, Scozzaro S, Sopena F, Lanas A, D'Haene N, Salmon I, Marine JC, Voet T, Sotiropoulou PA and Blanpain C. Identification of the tumour transition states occurring during EMT. Nature 2018; 556: 463-468.
[24] Okabe H, Satoh S, Kato T, Kitahara O, Yanagawa R, Yamaoka Y, Tsunoda T, Furukawa Y and Nakamura Y. Genome-wide analysis of gene expression in human hepatocellular carcinomas using cDNA microarray: identification of genes involved in viral carcinogenesis and tumor progression. Cancer Res 2001; 61: 2129-2137.
[25] Hsu CC, Shi J, Yuan C, Zhao D, Jiang S, Lyu J, Wang X, Li H, Wen H, Li W and Shi X. Recognition of histone acetylation by the GAS41 YEATS domain promotes H2A.Z deposition in non-small cell lung cancer. Genes Dev 2018; 32: 58-69.
[26] Sanchez-Garcia F, Villagrasa P, Matsui J, Kotliar D, Castro V, Akavia UD, Chen BJ, Saucedo-Cuevas L, Rodriguez Barrueco R, Llobet-Navas

D, Silva JM and Pe'er D. Integration of genomic data enables selective discovery of breast cancer drivers. Cell 2014; 159: 1461-1475.
[27] Barretina J, Taylor BS, Banerji S, Ramos AH, Lagos-Quintana M, Decarolis PL, Shah K, Socci ND, Weir BA, Ho A, Chiang DY, Reva B, Mermel CH, Getz G, Antipin Y, Beroukhim R, Major JE, Hatton C, Nicoletti R, Hanna M, Sharpe T, Fennell TJ, Cibulskis K, Onofrio RC, Saito T, Shukla N, Lau C, Nelander S, Silver SJ, Sougnez C, Viale A, Winckler W, Maki RG, Garraway LA, Lash A, Greulich H, Root DE, Sellers WR, Schwartz GK, Antonescu CR, Lander ES, Varmus HE, Ladanyi M, Sander C, Meyerson M and Singer S. Subtype-specific genomic alterations define new targets for soft-tissue sarcoma therapy. Nat Genet 2010; 42: 715-721.
[28] Dongre A and Weinberg RA. New insights into the mechanisms of epithelial-mesenchymal transition and implications for cancer. Nat Rev Mol Cell Biol 2019; 20: 69-84.
[29] Li Y, Wen H, Xi Y, Tanaka K, Wang H, Peng D, Ren Y, Jin Q, Dent SY, Li W, Li H and Shi X. AF9 YEATS domain links histone acetylation to DOT1L-mediated H3K79 methylation. Cell 2014; 159: 558-571.
[30] Cho HJ, Li H, Linhares BM, Kim E, Ndoj J, Miao H, Grembecka J and Cierpicki T. GAS41 recognizes diacetylated histone H3 through a bivalent binding mode. ACS Chem Biol 2018; 13: 2739-2746.
[31] Kimura H. Histone modifications for human epigenome analysis. J Hum Genet 2013; 58: 439-445.
[32] Sato Y, Hilbert L, Oda H, Wan Y, Heddleston JM, Chew TL, Zaburdaev V, Keller P, Lionnet T, Vastenhouw N and Kimura H. Histone H3K27 acetylation precedes active transcription during zebrafish zygotic genome activation as revealed by live-cell analysis. Development 2019; 146: dev179127.
[33] Chaffer CL, Marjanovic ND, Lee T, Bell G, Kleer CG, Reinhardt F, D'Alessio AC, Young RA and Weinberg RA. Poised chromatin at the ZEB1 promoter enables breast cancer cell plasticity and enhances tumorigenicity. Cell 2013; 154: 61-74.
[34] Wang Y, Wen M, Kwon Y, Xu Y, Liu Y, Zhang P, He X, Wang Q, Huang Y, Jen KY, LaBarge MA, You L, Kogan SC, Gray JW, Mao JH and Wei G. CUL4A induces epithelial-mesenchymal transition and promotes cancer metastasis by regulating ZEB1 expression. Cancer Res 2014; 74: 520-531.
[35] Prat A, Pineda E, Adamo B, Galván P, Fernández A, Gaba L, Díez M, Viladot M, Arance A and Muñoz M. Clinical implications of the intrinsic molecular subtypes of breast cancer. Breast 2015; 24 Suppl 2: S26-35.
[36] Gao JJ and Swain SM. Luminal A breast cancer and molecular assays: a review. Oncologist 2018; 23: 556-565.
[37] Park JH, Ahn JH and Kim SB. How shall we treat early triple-negative breast cancer (TNBC): from the current standard to upcoming immuno-molecular strategies. ESMO Open 2018; 3: e000357.
[38] Park JH and Roeder RG. GAS41 is required for repression of the p53 tumor suppressor pathway during normal cellular proliferation. Mol Cell Biol 2006; 26: 4006-4016.
[39] Huang G, Jiang H, Lin Y, Wu Y, Cai W, Shi B, Luo Y, Jian Z and Zhou X. lncAKHE enhances cell growth and migration in hepatocellular carcinoma via activation of NOTCH2 signaling. Cell Death Dis 2018; 9: 487.
[40] Wang SP, Wang WL, Chang YL, Wu CT, Chao YC, Kao SH, Yuan A, Lin CW, Yang SC, Chan WK, Li KC, Hong TM and Yang PC. p53 controls cancer cell invasion by inducing the MDM2-mediated degradation of Slug. Nat Cell Biol 2009; 11: 694-704.
[41] Park JH, Smith RJ, Shieh SY and Roeder RG. The GAS41-PP2Cbeta complex dephosphorylates p53 at serine 366 and regulates its stability. J Biol Chem 2011; 286: 10911-10917.
[42] Yang HD, Kim PJ, Eun JW, Shen Q, Kim HS, Shin WC, Ahn YM, Park WS, Lee JY and Nam SW. Oncogenic potential of histone-variant H2A.Z.1 and its regulatory role in cell cycle and epithelial-mesenchymal transition in liver cancer. Oncotarget 2016; 7: 11412-11423.
[43] Raisner R, Kharbanda S, Jin L, Jeng E, Chan E, Merchant M, Haverty PM, Bainer R, Cheung T, Arnott D, Flynn EM, Romero FA, Magnuson S and Gascoigne KE. Enhancer activity requires CBP/P300 bromodomain-dependent histone H3K27 acetylation. Cell Rep 2018; 24: 1722-1729.
[44] Liu B, Yang L, Zhu X, Li H, Zhu P, Wu J, Lu T, He L, Liu N, Meng S, Zhou L, Ye B, Tian Y and Fan Z. Yeats4 drives ILC lineage commitment via activation of Lmo4 transcription. J Exp Med 2019; 216: 2653-2668.

Supplementary materials and methods

Clinicopathological information in breast cancer patients

Estrogen receptor (ER), progesterone receptor (PR), human epidermal growth factor receptor 2 (HER2), and Ki-67 expression status were available from pathological reports. ER and PR were defined as positive with more than 10% positively staining nucleus [1]. Fluorescence *in situ* hybridization was performed to determine the HER2 status in the equivocal evaluation of HER2 expression by immunohistochemistry (IHC) [2]. The Ki-67 index was dichotomized to high- and low-expression groups, with 20% as the cut-off point [3]. Patients were staged using the American Joint Committee on Cancer (AJCC) for breast cancer staging [4]. All specimens were evaluated by two independent pathologists. Patient age, menstrual status, tumor size, histological grade, and lymph node status were obtained from medical records and pathological reports.

Breast cancer molecular subtypes

Patients were further classified based on surrogate definitions of ER, PR, HER2, and Ki-67 according to St. Gallen Consensus 2013 [5]: luminal A: ER-positive and/or PR-positive, HER2-negative, and Ki-67 ≤ 20%; luminal B (HER2-negative): ER-positive and/or PR-positive, HER2-negative, and Ki-67 > 20%; luminal B (HER2-positive): ER-positive and/or PR-positive, and HER2-positive; HER2 type: ER-negative, PR-negative, and HER2-positive; Triple-negative breast cancer (TNBC): ER-negative, PR-negative, and HER2-negative.

Lentiviral construction and cell infection

The short hairpin RNAs (shRNAs) targeting human YEATS4 and ZEB1 were designed and synthesized by GenePharma. The pLKO.1 constructed with specific shRNA and negative control shRNA (shCtrl), pCMVΔynthe, and pMD.G plasmids were co-transfected in 293T cells to package and produce lentivirus. Breast cancer cell lines were infected with the collected viral supernatant. The shRNA sequences are listed in Table S1. The plasmids of pcDNA3.1-control and pcDNA3.1-YEATS4 were transfected into cells by instantaneous transfection using X-tremeGENE™ HP DNA Transfection Reagent (Roche). A full-length coding sequence (CDS) of YEATS4 was implanted into the lentiviral vector pHIV-EGFP (Addgene) with an EF1-α promoter, a multiple cloning site (MCS), and EGFP. The lentiviral supernatant was obtained by transfecting 293T cells with pHIV-EGFP-YEATS4, pMDLg/pRRE, pMD2.G, and pRSV-Rev.

Cell proliferation assays

Cell proliferation was examined using the Cell Counting Kit-8 (CCK-8; Dojindo). Cells were cultured in 96-well plates (Corning) at a concentration of 2000 cells/well in a volume of 200 μL after stable YEATS4 deletion. At the indicated time points, 20 μL CCK-8 reagents were added to each well and then incubated for 2 h at 37°C. The absorbance at 450 nm was measured with a microplate reader. Each independent experiment was repeated three times.

Colony formation and soft agar colony formation assays

Colony formation assays: Cells stably transfected with OSR1-shRNAs or stably OSR1-expressing cells were digested into single cells, which were cultured in a 6-well plate with a density of 1×10^3 cells per well with 5% CO_2 at 37°C for 2 weeks. After colony formation, the plate was gently rinsed with PBS, fixed with 4% paraformaldehyde for 20 min, and stained with 0.2% crystal violet for 10 min. Colonies composed of more than 50 cells were then counted for the colony-forming assays. Three independent assays were performed to confirm the results.

Soft agar colony formation assays: The tested cells (1×10^3) were grown in 1 mL of complete medium containing 0.3% low-melting-point agarose gel (Sigma-Aldrich) and rested on another layer of 1.5 mL of 0.6% agarose gel in 6-well plates. The cells were then incubated with 5% CO_2 at 37°C for 2 weeks. Colonies larger than 50 μm in diameter were observed and counted under the microscope. Three independent experiments were performed to confirm the results.

Wound healing assays

Cells were cultured in 6-well plates (Corning) to reach more than 90% confluency in a monolayer. The scratched wounds were made using a sterile 200 μL pipette tip in the cell monolayer. The wells were rinsed with PBS to remove cellular fragments and incubated with 5% CO_2 at 37°C. Images were then taken with an optical microscope. The cell migrating distance was measured by gauging the scratch space at 0 h, 24 h, and 48 h by using the ImageJ software. Each independent experiment was repeated three times.

Transwell assays

For the invasion assays, breast cancer cells (2×10^4 cells) in a serum-free medium were plated into transwell chambers (8 μm pore size; Corning) coated with 60 μL of Matrigel (1:8 dilution; BD Biosciences). For cell migration assays, no Matrigel was added. The culture medium containing 20% FBS was filled in the lower compartment as a chemical attractant. After incubation for 24-48 h, the cells in the upper chamber were removed with a cotton tip. The cells on the bottom side of the transwell membrane were fixed with 4% paraformaldehyde for 20 min and stained with 0.25% crystal violet staining solution for 30 min. The cells were photographed with an optical microscope. The number of cells passing through the membrane in five random fields was determined using the ImageJ software. Each independent experiment was repeated three times.

Western blot analysis

Cellular protein was extracted using RIPA buffer (Sigma-Aldrich). Protein concentrations were quantified using the Bicinchoninic Acid Kit (Sigma-Aldrich) as instructed by the manufacturer. Proteins were resolved using 10% SDS-PAGE gel electrophoresis. They were then transferred to a polyvinylidene fluoride membrane (Millipore), blocked in 5% non-fat milk (Sigma-Aldrich) for 2 h, and incubated with the primary antibody (anti-YEATS4, Sigma-Aldrich, diluted by 1:1000; anti-GAPDH, Cell Signaling Technology, diluted by 1:1000) at 4°C overnight. Membranes were then incubated with the HRP-linked secondary antibody (diluted by 1:2000; Cell Signaling Technology) for 1 h at room temperature. Blots were visualized by using an ECL Detection Kit (Millipore) and analyzed using the ImageJ software.

Immunofluorescence

Cells growing on glass cover slides were fixed with 4% paraformaldehyde for 15 min at room temperature, permeated with PBS containing 0.25% Triton X-100 for 30 min, blocked with 1% BSA for 1 h at room temperature, and incubated overnight with the indicated primary antibodies at 4°C and then with fluorescence-conjugated secondary antibodies. Nuclei were stained with DAPI. Cells were visualized by confocal laser scanning microscopy (Zeiss LSM 880).

Dual luciferase reporter assays

Luciferase reporter assays were conducted in accordance with the instructions provided by the manufacturer. The ZEB1 promoter was inserted into the pGL3-Basic luciferase expression vector (Genepharma). Cells were grown in 12-well plates (Corning) and transfected with an appropriate pcDNA3.1 plasmid, together with a luciferase plasmid, by using the X-tremeGENE HP DNA Transfection Reagent (Roche). After transfection for 48 h, cell lysates were obtained and luciferase reporter activities were measured using the Dual-Luciferase Reporter System (Promega). Firefly luciferase activities were normalized to the activities of Renilla luciferase as the control. Each experiment was repeated three times.

In vivo tumorigenicity and metastasis assays

Female athymic nude mice (BALB/c-nu/nu) aged 4-6 weeks were obtained from Shanghai SLAC Laboratory Animal Company (Shanghai, China) and kept in specific-pathogen-free (SPF) environments at the Experimental Animal Center of Shanghai General Hospital, Shanghai Jiao Tong University School of Medicine. For tumorigenicity assays, tumor cells were resuspended in phosphate-buffered saline (PBS)

at a concentration of 2×10^6/100 μL and injected subcutaneously into the nude mice (n = 6 for each group). The xenograft tumor size was evaluated every 3 d with a Vernier caliper. Tumor volume was calculated using the following formula: volume (mm^3) = [(shortest length)^2 × longest length]/2. Growth curves were plotted and analyzed for every group. All mice were euthanized after 40 d to isolate and collect tumors. The tumor weight was measured and recorded. For lung metastasis assays, tumor cells were resuspended in PBS at a density of 2×10^6/100 μL and intravenously injected into the nude mice (n = 8 for each group). The survival of all mice was recorded throughout the experiment. After 9 weeks, all mice were euthanized, and their lungs were resected for standard histological examinations.

References

[1] Yip CH and Rhodes A. Estrogen and progesterone receptors in breast cancer. Future Oncol 2014; 10: 2293-2301.

[2] Elebro K, Bendahl PO, Jernström H and Borgquist S. Androgen receptor expression and breast cancer mortality in a population-based prospective cohort. Breast Cancer Res Treat 2017; 165: 645-657.

[3] Coates AS, Winer EP, Goldhirsch A, Gelber RD, Gnant M, Piccart-Gebhart M, Thürlimann B and Senn HJ. Tailoring therapies--improving the management of early breast cancer: St gallen international expert consensus on the primary therapy of early breast cancer 2015. Ann Oncol 2015; 26: 1533-1546.

[4] Giuliano AE, Connolly JL, Edge SB, Mittendorf EA, Rugo HS, Solin LJ, Weaver DL, Winchester DJ and Hortobagyi GN. Breast cancer-major changes in the American joint committee on cancer eighth edition cancer staging manual. CA Cancer J Clin 2017; 67: 290-303.

[5] Goldhirsch A, Winer EP, Coates AS, Gelber RD, Piccart-Gebhart M, Thürlimann B and Senn HJ. Personalizing the treatment of women with early breast cancer: highlights of the St gallen international expert consensus on the primary therapy of early breast cancer 2013. Ann Oncol 2013; 24: 2206-2223.

Table S1. ShRNA and primer sequences used in the research

Application	Gene	Sequence
Small hairpin RNA (shRNA)	YEATS4 #1	GCGGGAGAGTAAAGGGTGTTA
		TAACACCCTTTACTCTCCCGC
	YEATS4 #2	GGGAGAGTAAAGGGTGTTACT
		AGTAACACCCTTTACTCTCCC
	ZEB1	GGAGGATAAAGAGATGGAAGA
		TCTTCCATCTCTTTATCCTCC
Real time quantitative polymerase chain reaction (RT-qPCR)	YEATS4	GAGAATGGCCGAATTTGGGC
		CCGAGCAACATTACCGTAAACT
	Snail	ACTGCGACAAGGAGTACACC
		GAGTGCGTTTGCAGATGGG
	Slug	CGAACTGGACACACATACAGTG
		CTGAGGATCTCTGGTTGTGGT
	Twist1	GTCCGCAGTCTTACGAGGAG
		GCTTGAGGGTCTGAATCTTGCT
	ZEB1	GATGATGAATGCGAGTCAGATGC
		ACAGCAGTGTCTTGTTGTTGT
	FOXC2	CCTCCTGGTATCTCAACCACA
		GAGGGTCGAGTTCTCAATCCC
	EZH2	AATCAGAGTACATGCGACTGAGA
		GCTGTATCCTTCGCTGTTTCC
	BMI1	CGTGTATTGTTCGTTACCTGGA
		TTCAGTAGTGGTCTGGTCTTGT
	E-cadherin	CGAGAGCTACACGTTCACGG
		GGGTGTCGAGGGAAAAATAGG
	ZO-1	CAACATACAGTGACGCTTCACA
		CACTATTGACGTTTCCCCACTC
	Vimentin	GACGCCATCAACACCGAGTT
		CTTTGTCGTTGGTTAGCTGGT
	N-cadherin	TTTGATGGAGGTCTCCTAACACC
		ACGTTTAACACGTTGGAAATGTG
	E47	ACGAGCGTATGGGCTACCA
		GTTATTGCTTGAGTGATCCGGG
	GAPDH	TGTGGGCATCAATGGATTTGG
		ACACCATGTATTCCGGGTCAAT
ChIP assays	ZEB1 site A	TATTCGAAGGAGGTGGGAAGCAGG
		CGTGCAGGACCTTAAGGCAAGAAG
	ZEB1 site B	ACCGCTGATGAACTTTCCCA
		TGGAACTACCACAACGAGGC
	ZEB1 site C	CGTCCCCTAAGGCCAATACC
		AGCGTATGCATTTCGTTGCC

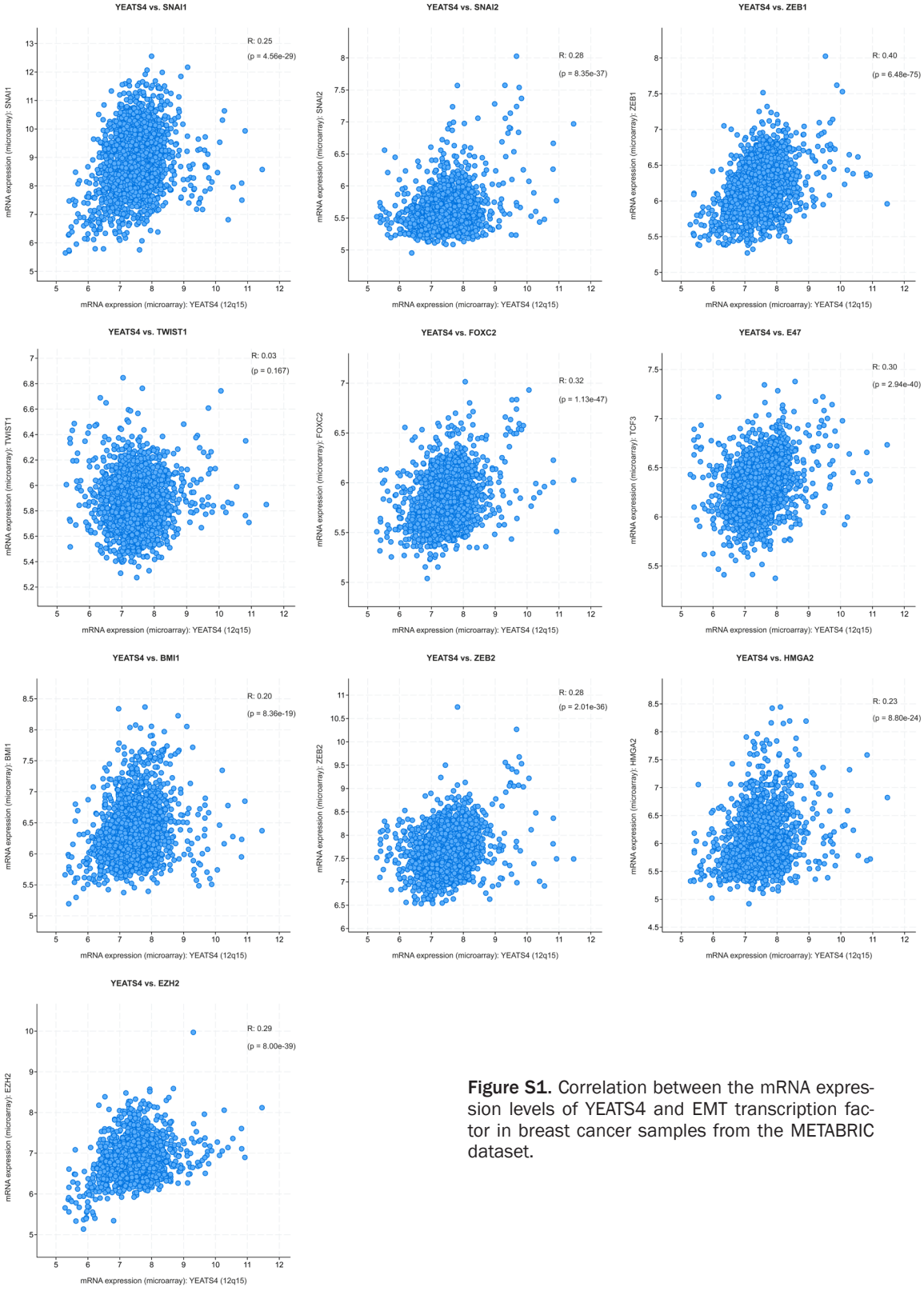

Figure S1. Correlation between the mRNA expression levels of YEATS4 and EMT transcription factor in breast cancer samples from the METABRIC dataset.

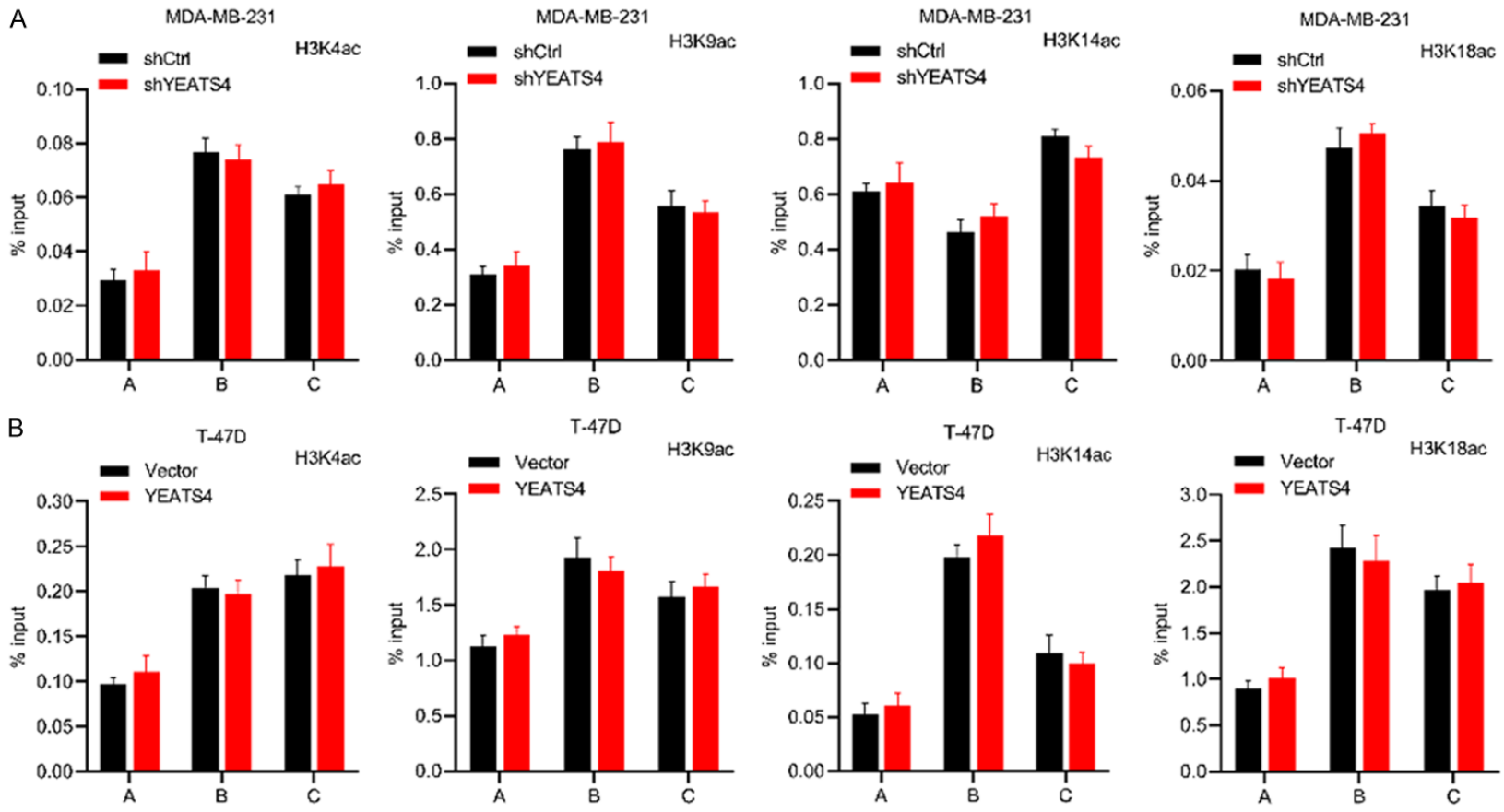

Figure S2. ChIP assays were performed to determine H3K4ac, H3K9ac, H3K14ac, and H3K18ac occupancy in MDA-MB-231-shYEATS4 (A) and T-47D-YEATS4 (B) cells. Data were presented as mean ± standard deviation for 3 independent assays.

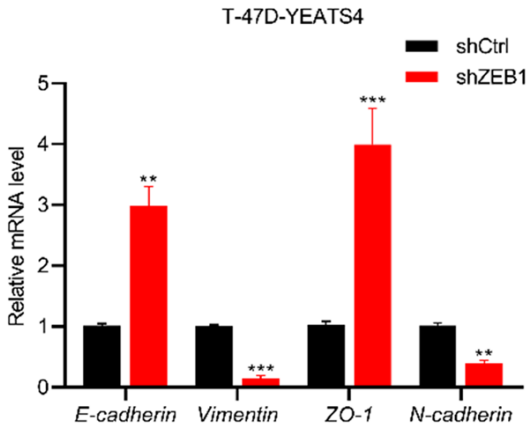

Figure S3. Deleting ZEB1 restored the expression of the epithelial markers E-cadherin and ZO-1 and reduced the mesenchymal markers vimentin and N-cadherin in T-47D-YEATS4 cells, as determined by real-time quantitative polymerase chain reaction (RT-qPCR). Data were presented as mean ± standard deviation for 3 independent assays. **, $P < 0.01$; ***, $P < 0.001$.